JAERI-Tech
96-042

DESIGN OF INTERMEDIATE HEAT EXCHANGER FOR THE HTGR-CLOSED CYCLE GAS TURBINE POWER GENERATION SYSTEM

October 1996

Yasushi MUTO, Kazuhiko HADA
Hajime KOIKEGAMI* and
Hiroyuki KISAMORI*

日本原子力研究所
Japan Atomic Energy Research Institute

本レポートは，日本原子力研究所が不定期に公刊している研究報告書です。
入手の問合わせは，日本原子力研究所研究情報部研究情報課（〒319-11 茨城県那珂郡東海村）あて，お申し越しください。なお，このほかに財団法人原子力弘済会資料センター（〒319-11 茨城県那珂郡東海村日本原子力研究所内）で複写による実費頒布をおこなっております。

This report is issued irregularly.
Inquiries about availability of the reports should be addressed to Research Information Division, Department of Intellectual Resources, Japan Atomic Energy Research Institute, Tokai-mura, Naka-gun, Ibaraki-ken 319-11, Japan.

編集兼発行　日本原子力研究所
印　　刷　日立高速印刷株式会社

Design of Intermediate Heat Exchanger for the HTGR-closed Cycle Gas Turbine Power Generation System

Yasushi MUTO, Kazuhiko HADA, Hajime KOIKEGAMI *
and Hiroyuki KISAMORI *

Department of Advanced Nuclear Heat Technology
Tokai Research Establishment
Japan Atomic Energy Research Institute
Tokai-mura, Naka-gun, Ibaraki-ken
(Received September 20 , 1996)

High thermal efficency can be achieved in a power generation system, which couples a high-temperature gas-cooled reactor(HTGR) with a closed cycle gas turbine(GT). There are three possible systems such as a direct cycle(DC), an indirect cycle(IDC) and an indirect gas-steam combined cycle(IDCC). An intermediate heat exchanger(IHX) is needed in the IDC or in the IDCC. However, the size of IHX is too large for a reasonable design and it has become one of the most important issues. Then, a design has been undertaken based on the experience of the IHX in the HTTR though as a material of heat transfer tubes, a Ni-Cr-W superalloy with the highest strength at temperature was adopted instead of Hastelloy XR used in the HTTR. First, by parametric design studies, the optimum design parameters have been examined for a heat duty of 150MW. Then, the IHX of 315 MW has been designed specifically and its dimensions and structures were determined. The IHX was clarified to be capable of fabrication at least in the case of IDCC. The results of parametric studies are useful to make a rough estimate for the other cases and some examples are shown.

Keywords : IHX, Intermediate Heat Exchanger, HTGR, Gas Turbine, Closed Cycle, Helium Turbine, Indirect Cycle, Ni-Cr-W Superalloy, Gas Turbine Power Generation, Cooling Component, High Temperature Gas-cooled Reactor, Heat Exchanger.

*Ishikawajima-Harima heavy Industries Co.,Ltd.

HTGR－閉サイクルガスタービン発電システム用中間熱交換器の設計

日本原子力研究所東海研究所核熱利用研究部
武藤　康・羽田　一彦・小池上　一*・木佐森演行*

（1996年9月20日受理）

高温ガス炉（HTGR）を閉サイクルガスタービンに接続する発電システムにより高い熱効率が期待できる。直接サイクル（DC），間接サイクル（IDC），間接ガス－蒸気複合サイクル（IDCC）の３種類のサイクル形式が考えられる。IDC及びIDCCにおいては中間熱交換器（IHX）を必要とするが，IHXの寸法が過大となり，合理的な設計が出来なくなるという懸念があり，最も重要な検討課題となっている。そこで，HTTRにおけるIHXの設計経験に基づき設計を試みた。ただし，伝熱管の材料としては，HTTRのハステロイXRに替えて最も高温強度の高いNi－Cr－W超合金を使用した。先ず，伝熱量150MWの場合について，パラメトリックに設計検討を行い，最適設計パラメータを求めた。次に，315MWのIHXについて詳細な設計を行い，寸法及び構造を決定した。この結果，少なくともIDCCの場合においてはIHXは製作可能であることが明らかにされた。また，パラメータ・サーベイの結果は他のケースの寸法の概算に有効であり，幾つかの具体例を示した。

東海研究所：〒319－11　茨城県那珂郡東海村白方白根２－４
＊石川島播磨重工業（株）

Contents

目　　次

1. Introduction

It is expected that a high thermodynamic thermal efficiency of 50% can be achieved in a HTGR-GT power generation system coupling a high-temperature gas-cooled reactor(HTGR) with a closed cycle gas turbine(GT). That means an effective reduction in the amount of waste heat, radioactive waste and nuclear fuel resource and is thought to be the most useful power generation system to provide a safer environment. Moreover, it has recently been shown in the design work[1] conducted by Gas-Cooled Reactor Associates(GCRA) that the system is competitive enough compared with the advanced light-water reactor(ALWR) and natural gas combined cycle combustion turbine(CCCT).

In the HTGR-GT system, the high-temperature helium gas leaving a reactor flows into a gas turbine and expands. After that, it flows through a recuperator and a precooler and is compressed at the compressor and goes back to the reactor via the recuperator. The system is called the direct cycle (DC). Though it has the high possibility of attaining both high thermal efficiency and low cost, there are some difficulties that need to be overcome.

The first problem is that the reactor outlet helium gas contains a small amount of fission products, some of which are vapor fission products such as Cs, Sr and Ag and deposit on the surface of turbo-machinery. Though the amount of fission products are small, the resultant radioactivity after 30 to 40 year's operation becomes too high to be accessible for maintenance.

The second problem is that the turbo-machinery, the recuperator and the precooler must be installed in a pressure vessel called a power conversion vessel (PCV). As the available space in the pressure vessel is limited, more compact recuperator and precooler are needed than feasible using the current technology.

The third problem is that the optimum temperature of returning helium gas to the reactor becomes around 500°C which is higher than a proven 400°C of the high-temperature engineering test reactor(HTTR) now under construction at Oarai in Japan[2] and requires a new vessel material like 9Cr-1Mo-V steel.

An indirect cycle (IDC) can solve the first and second problems where the reactor outlet helium gas transfers its heat to a secondary helium gas flowing in a turbine loop via an intermediate heat exchanger(IHX). Though the maintenance of turbo-machines becomes easier and the dimensional limits confronting the recuperator and precooler are lessen, new problems appear. The size of IHX is too large. The reactor inlet temperatue is still required to be 500°C or greater and a significant reduction in the thermal efficiency

is inevitable. To solve these problems, an indirect combined gas-turbine cycle (IDCC) is proposed where a topping cycle is the Brayton cycle and a bottoming cycle is the Rankine-steam cycle. The IDCC makes use of the steam cycle instead of a recuperator to achieve a high thermal efficiency. By this means, the temperature of returning He gas to IHX, and then, the reactor can be kept below 400°C which is suitable for the use of CrMo or MnMo steel. The IDCC is classified into two types, that is, a perfect cascade type and a semi-cascade type as shown in Fig.1[2]. Features of the perfect cascade type is essentially the same as the simple indirect cycle except for the reactor inlet temperature. On the other hand, the semi-cascade type has an additional benefit. In this configuration, a boiler for the steam cycle is provided in the primary circuit at the downstream of IHX. Such a configuration is effective to reduce the size of IHX because the higher logarithmic mean temperature difference(ΔTm) is obtained and the heat duty of IHX is reduced.

In this report, it is examined based on parametric design studies how large the sizes of IHX for both the perfect cascade type and semi-cascade type of IDCC become. Then, the design data and the arrangement for the IHX with a heat duty of 315 MW are given.

2. System Design

A reactor thermal output of 450 MW was set, which is based on the design of GCRA[1]. As the outlet He gas temperature, 950 and 900°C were selected. The former corresponds to that of HTTR[3] and is the highest temperature which has been achieved so far. As for helium gas pressure, 8 MPa was chosen which was a little higher than that of GCRA design.

Three cases were considered. Case 1 is a perfect cascade type with a reactor outlet temperature of 950°C. Cases 2 and 3 are semi-cascade types whose reactor outlet temperature are 950 and 900°C, respectively. The case 3 of 900°C was taken up to examine a trade-off between a merit due to a higher strength of material facilitating a structural design and a demerit due to a reduction of thermal cycle efficiency.

Figure 2 shows materials and heat balance in case 1. The 2ry He gas outlet temperature of 910°C was selected so as to attain the minimum hot leg approach temperature of 40°C necessary for the heat transmission. In this case, a heat duty of IHX is almost equal to the thermal output of the reactor. Though 8 MPa of the steam pressure was set, this value might be arbitrarily selected in this case. Since the thermal cycle efficiency of the steam cycle increases in accordance with the increase in steam pressure, a

is inevitable. To solve these problems, an indirect combined gas-turbine cycle (IDCC) is proposed where a topping cycle is the Brayton cycle and a bottoming cycle is the Rankine-steam cycle. The IDCC makes use of the steam cycle instead of a recuperator to achieve a high thermal efficiency. By this means, the temperature of returning He gas to IHX, and then, the reactor can be kept below 400°C which is suitable for the use of CrMo or MnMo steel. The IDCC is classified into two types, that is, a perfect cascade type and a semi-cascade type as shown in Fig.1[2]. Features of the perfect cascade type is essentially the same as the simple indirect cycle except for the reactor inlet temperature. On the other hand, the semi-cascade type has an additional benefit. In this configuration, a boiler for the steam cycle is provided in the primary circuit at the downstream of IHX. Such a configuration is effective to reduce the size of IHX because the higher logarithmic mean temperature difference(ΔTm) is obtained and the heat duty of IHX is reduced.

In this report, it is examined based on parametric design studies how large the sizes of IHX for both the perfect cascade type and semi-cascade type of IDCC become. Then, the design data and the arrangement for the IHX with a heat duty of 315 MW are given.

2. System Design

A reactor thermal output of 450 MW was set, which is based on the design of GCRA[1]. As the outlet He gas temperature, 950 and 900°C were selected. The former corresponds to that of HTTR[3] and is the highest temperature which has been achieved so far. As for helium gas pressure, 8 MPa was chosen which was a little higher than that of GCRA design.

Three cases were considered. Case 1 is a perfect cascade type with a reactor outlet temperature of 950°C. Cases 2 and 3 are semi-cascade types whose reactor outlet temperature are 950 and 900°C, respectively. The case 3 of 900°C was taken up to examine a trade-off between a merit due to a higher strength of material facilitating a structural design and a demerit due to a reduction of thermal cycle efficiency.

Figure 2 shows materials and heat balance in case 1. The 2ry He gas outlet temperature of 910°C was selected so as to attain the minimum hot leg approach temperature of 40°C necessary for the heat transmission. In this case, a heat duty of IHX is almost equal to the thermal output of the reactor. Though 8 MPa of the steam pressure was set, this value might be arbitrarily selected in this case. Since the thermal cycle efficiency of the steam cycle increases in accordance with the increase in steam pressure, a

higher thermal efficiency could be expected.

Figure 3 shows materials and heat balance in case 2. The secondary He gas inlet temperature is also 910°C. In this case, a steam boiler is provided at a cold leg of IHX. This configuration enables a reduction in the heat duty of IHX to 2/3, and at the same time, a logarithmic temperature difference is significantly magnified because of both a higher primary He gas outlet temperature and a lower secondary He gas inlet temperature. The latter became possible since the limit of pinch point was mitigated. In this case, the increase in steam pressure needs a careful examination on the water ingress accident due to the failed boiler tubes.

Figure 4 shows materials and heat balance in case 3. This case is similar to case 2 except that a gas turbine inlet temperature is lower, and therefore, the thermal cycle efficiency is about 2% lower.

The parameters needed for the design of IHX are listed in Table 1 where thermal cycle efficiencies are also shown.

3. Material Data of Ni-Cr-W Superalloy

A Ni-Cr-W superalloy[4] was selected as the material for the high-temperature parts such as the heat transfer tubes, a tube header and a center pipe for IHX. The superalloy has been developed by the Subcommittee on Advanced Superalloys of the Technical Expert Committee on HTGR at the Japan Atomic Energy Research Institute. It consists of 19% Cr, 21% W, 59% Ni and many kinds of miner elements such as C, Ti, Zr, Y and B. It is strenghtened by means of a precipitation of the α_2 W phase and has the highest creep strength at 950°C among all forged alloys.

The superalloy is still under development and limited data are available. Generally, the stress-rupture data are dependent on product forms such as a forged plate, a forged bar and a drawn tube. In the case of the Ni-Cr-W superalloy, the experimental data showed that the strength for the tube was equivalent to that for the forged bar at 900°C, but lower than at 1000°C. In addition, the So value necessary for the sizing requires not only stress-rupture data but also minimum creep strain rate data which are not available. Then, So value was estimated by means of multiplying the experimental stress-rupture strength for the forged bar by a reduction factor of 0.9 to compensate the uncertain effects of both the tube-form and minimum creep rate. The results are shown in Table 2. Figure 5 compares this So value with those for Hastelloy XR and Inconel 617. The values of Hastelloy XR are those used in the HTTR IHX[5]. Those of Inconel 617 are calculated from the St data[6] corresponding to 10^5 h.

higher thermal efficiency could be expected.

Figure 3 shows materials and heat balance in case 2. The secondary He gas inlet temperature is also 910°C. In this case, a steam boiler is provided at a cold leg of IHX. This configuration enables a reduction in the heat duty of IHX to 2/3, and at the same time, a logarithmic temperature difference is significantly magnified because of both a higher primary He gas outlet temperature and a lower secondary He gas inlet temperature. The latter became possible since the limit of pinch point was mitigated. In this case, the increase in steam pressure needs a careful examination on the water ingress accident due to the failed boiler tubes.

Figure 4 shows materials and heat balance in case 3. This case is similar to case 2 except that a gas turbine inlet temperature is lower, and therefore, the thermal cycle efficiency is about 2% lower.

The parameters needed for the design of IHX are listed in Table 1 where thermal cycle efficiencies are also shown.

3. Material Data of Ni-Cr-W Superalloy

A Ni-Cr-W superalloy[4] was selected as the material for the high-temperature parts such as the heat transfer tubes, a tube header and a center pipe for IHX. The superalloy has been developed by the Subcommittee on Advanced Superalloys of the Technical Expert Committee on HTGR at the Japan Atomic Energy Research Institute. It consists of 19% Cr, 21% W, 59% Ni and many kinds of miner elements such as C, Ti, Zr, Y and B. It is strenghtened by means of a precipitation of the α_2 W phase and has the highest creep strength at 950°C among all forged alloys.

The superalloy is still under development and limited data are available. Generally, the stress-rupture data are dependent on product forms such as a forged plate, a forged bar and a drawn tube. In the case of the Ni-Cr-W superalloy, the experimental data showed that the strength for the tube was equivalent to that for the forged bar at 900°C, but lower than at 1000°C. In addition, the So value necessary for the sizing requires not only stress-rupture data but also minimum creep strain rate data which are not available. Then, So value was estimated by means of multiplying the experimental stress-rupture strength for the forged bar by a reduction factor of 0.9 to compensate the uncertain effects of both the tube-form and minimum creep rate. The results are shown in Table 2. Figure 5 compares this So value with those for Hastelloy XR and Inconel 617. The values of Hastelloy XR are those used in the HTTR IHX[5]. Those of Inconel 617 are calculated from the St data[6] corresponding to 10^5 h.

The value of specific gravity is 9.35 which is a measured one[7]. No data are available regarding thermal conductivity. Then, the data shown in Table 3 for the analogous W material[8] were used.

4. Parametric Sizing Study

4.1 Sizing procedure and design conditions

Figure 6 shows the sizing procedure. First, a design temperature, a design pressure, the other design loads are assumed. Under these design conditions, both a diameter and thickness of tube are determined so as to meet the stress limits. Then, under the assumption of both a heat duty and a number of tubes, heat transfer computations are carried out and a tube length is determined. Pressure drops are computed for the given tube length. Finally, the optimum point is selected within the assumed limiting conditions.

Design temperature is determined as follows. The maximum operating temperature of the metal of the heat transfer tube is assumed to be an average of temperatures of the primary He gas and secondary He gas. Regarding this value, a margin of 30°C which consists of a measurement error, a control range and so on, are superposed. Therefore, the design temperature becomes 960 and 905°C for cases 1 and 2 and 3, respectively.

The design pressure is determined as follows. The maximum pressure difference is calculated by subtracting the primary He gas outlet pressure from the secondary He gas inlet pressure. As an IHX is designed by not the total pressure but the pressure difference, the design pressure is determined by adding a margin consisting of a control range and a redundancy on the maximum pressure difference. In these cases, the maximum pressure difference is 0.35 MPa and the margin is 0.14 MPa, and then, the design pressure becomes 0.49 MPa.

4.2 Sizing of heat transfer tubes

Two cases, that is, ϕ31.8 mm and ϕ25.4 mm, have been examined for the outer diameter. The material of heat transfer tubes is Ni-Cr-W superalloy and So value prepared in Chapter 3 were used. The conformity to the general primary-membrane stress intensity limit is evaluated by the design pressure. The conformity to combined primary-membrane-plus-bending stress intensities limit is evaluated by a bending stress due to the dead load, which reaches its maximum at the connecting tube between the helical coil section and the tube header. In the case of an outer diameter of ϕ31.8 mm, the bending moment due to the dead load was assumed to be 19.6 Nm which was 5 times as

The value of specific gravity is 9.35 which is a measured one[7]. No data are available regarding thermal conductivity. Then, the data shown in Table 3 for the analogous W material[8] were used.

4. Parametric Sizing Study

4.1 Sizing procedure and design conditions

Figure 6 shows the sizing procedure. First, a design temperature, a design pressure, the other design loads are assumed. Under these design conditions, both a diameter and thickness of tube are determined so as to meet the stress limits. Then, under the assumption of both a heat duty and a number of tubes, heat transfer computations are carried out and a tube length is determined. Pressure drops are computed for the given tube length. Finally, the optimum point is selected within the assumed limiting conditions.

Design temperature is determined as follows. The maximum operating temperature of the metal of the heat transfer tube is assumed to be an average of temperatures of the primary He gas and secondary He gas. Regarding this value, a margin of 30°C which consists of a measurement error, a control range and so on, are superposed. Therefore, the design temperature becomes 960 and 905°C for cases 1 and 2 and 3, respectively.

The design pressure is determined as follows. The maximum pressure difference is calculated by subtracting the primary He gas outlet pressure from the secondary He gas inlet pressure. As an IHX is designed by not the total pressure but the pressure difference, the design pressure is determined by adding a margin consisting of a control range and a redundancy on the maximum pressure difference. In these cases, the maximum pressure difference is 0.35 MPa and the margin is 0.14 MPa, and then, the design pressure becomes 0.49 MPa.

4.2 Sizing of heat transfer tubes

Two cases, that is, ϕ31.8 mm and ϕ25.4 mm, have been examined for the outer diameter. The material of heat transfer tubes is Ni-Cr-W superalloy and So value prepared in Chapter 3 were used. The conformity to the general primary-membrane stress intensity limit is evaluated by the design pressure. The conformity to combined primary-membrane-plus-bending stress intensities limit is evaluated by a bending stress due to the dead load, which reaches its maximum at the connecting tube between the helical coil section and the tube header. In the case of an outer diameter of ϕ31.8 mm, the bending moment due to the dead load was assumed to be 19.6 Nm which was 5 times as

large as that in HTTR, on account of the effect due to the larger coil diameter. Here, the effect of the wall thickness to the weight of tube was not reckoned. As the dimmension of tube in the HTTR is φ31.8 mm × t3.5 mm, the results are strictly valid only for a thickness of t3.5 mm. Though such an estimation of moment seems to be somewhat rough, it will be strict enough for the objective of a parametric study. In the case of the outer diameter of φ25.4 mm, the value of 15.7 Nm was assumed which was 0.8 times as large as that of φ31.8 mm.

Figures 7 and 8 show the calculated stress intensities depending on a wall thickness in the cases of 960 and 905°C, respectively.

By the way, the following relationships exist between stress intensities and a wall thickness.

$$P_m = \frac{Pd_m}{2t}$$

$$P_L + P_b = \frac{Pd_m}{2t} + \frac{10^3 M}{0.8 d_m^2 t}$$

where P_m = general primary membrane stress intensity (MPa),
P_L = local primary membrane stress intensity (MPa),
P_b = primary bending stress intensity (MPa),
P = design pressure (MPa),
M = bending moment (Nm),
d_m = average diameter (mm),
t = wall thickness (mm).

The hyperbolic lines shown in figures show these relationships.

In cases 1 and 2 at 960°C, φ31.8 × t3.2 mm was selected. However, though the stress intensity $P_L + P_b$ exceeds the limit a little for the thickness of 2.6 mm, a selection of this value will be possible because the dead load itself is smaller in 2.6 mm than in 3.2 mm thicknesses. The outer diameter of 25.4 mm is unacceptable because a wall thickness of more than 4 mm is required.

On the other hand, both values of φ31.8 mm × t2.6 mm and φ25.4 mm × t2.6 mm were selected for the examination of heat transfer characteritics.

4.3 Heat transfer and fluid dynamic characteristics

A heat duty of the IHX was assumed to be 150 MW for the parametric study. The heat duties for cases 1 and 2 can be obtained by multiplying 150

MW by 3 and 2, respectively. Under this assumption, dependences of heat transfer characteristics such as a gas velocity, a heat transfer coefficient and a coil length and also a pressure drop on the number of tubes have been calculated as follows.

Step 1. Assuming the number of tubes, a diameter of helical coil shown in Fig. 9 and a flow area are determined since a radial pitch of tube is constant.

Step 2. The secondary (tube side) He gas velocity shown in Fig. 10 and the primary (shell side) He gas velocity shown in Fig. 11 are determined since the mass flow rate is given for each case. Naturally, the gas velocity is reduced as a number of tubes increases:

$$v = \frac{G}{\rho A_f}$$

where v = gas velocity (m/s)
G = mass flow rate (kg/s)
ρ = density (kg/m^3)
A_f = flow area (m^2)

Step 3. When a gas velocity is determined, a heat transfer coefficient, and then, the overall heat transfer coefficient can be calculated. A required heat transfer area is obtained by the next equation as shown in Fig. 12:

$$F = \frac{Q}{\Delta T_m K}$$

where F = heat transfer area (m^2)
Q = heat duty (MW)
ΔT_m = Logarithmic mean temperature difference (°C)
K = Overall heat transfer coefficient ($MW/m^2 °C$)

Step 4. The tube length, and then, a coil height shown in Fig. 13 are determined since the number of tubes and the inclination angle are assumed:

$$L = \frac{F}{n\pi d}$$

where L = tube length (m)
n = number of tubes
d = reference diameter of tube for the heat transfer calculation (m)

Step 5. When a length of tube is determined, pressure drops are

calculated. A tube side pressure drop and a shell side pressure drop are shown in Figs. 14 and 15, respectively.

Using these figures, an appropriate value can be selected under the following limitations:

(a) Tube side gas velocity < 50 m/s
(b) Shell side gas velocity < 15 m/s
(c) Tube side total pressure drop ($\Delta p/p$) < 1.6 %
(d) Shell side total pressure drop ($\Delta p/p$) < 1.6 %

where the pressure drop of the effective heat transfer section (helical coil section) was assumed to be 80% of the total pressure drop. The value of 50m/s has been assumed based on the existing data for a gas to gas heat exchanger. The limit of 15 m/s has been assumed to prevent a flow induced vibration. The upper limits of the pressure drop have been assumed based on those in the reference[9].

Comparing those limits with the calculated values, the values of shell side pressure drop is sufficiently less than the limit in every case. In addition, if we select the number of tubes so as to conform to the limit of tube side pressure drop, the limit of tube side gas velocity is also satisfied (though there is some amount of discrepancy as far as case 1 is concerned). Therefore, it is sufficient to select a value to meet only the limits of both tube side pressure drops and the shell side gas velocity.

Now, comparing case 1 (Perfect cascade type) with case 2 (Semi-cascade type), secondary (tube side) gas velocity of case 1 is a little higher than that of case 2 as shown in Fig. 10. On the other hand, primary (shell side) gas velocity is 67% of case 2 as shown in Fig. 11. This is attributed mainly to the substantial difference of the mass flow rate per 150 MW though there is an effect due tothe difference of density caused by the difference of temperature and pressure (see the figures in the parenthesis of Table 1). The heat transfer coefficient is proportional to 0.8th power of the gas velocity (Reynolds number). As the shell side gas velocity governs the overall heat transfer coefficient, which in case 1 becomes 73% of case 2 ($0.67^{0.8}=0.73$), and consequently, results in the corresponding increase in heat transfer area in case 1. By the way, the heat transfer area of case 1 is 4 times larger than that of the other cases as shown in Fig. 12. The difference is far beyond the amount expected from the difference of heat transfer coefficient. This is caused by the very small value of the assumed logarithmic mean temperature difference, that is, 40°C (see Table 1). For the given number of tubes, this means the longer tube length, which is observed in Fig. 13. This leads to an increase in the tube side pressure

drop. Since the tube side pressure drop exceeds the allowable limit, an increase in the number of tubes is required in case 1. In case 3 (reactor outlet temperature = 900°C), the heat transfer areas become somewhat smaller compared with case 2 in the outer diameter of φ31.8 mm and also φ25.4 mm.

Table 4 shows a summary of the parametric sizing study. Here, the values of the heat exchange capacities do not coinside with just 150 MW, because of the convenience of calculation. Though there are some variations due to the limit of the sizing, it can be observed that the dimmensions of case 1 is much larger than those of the other cases in both the number of coil layers and coil height. There is no significant difference in the dimmensions between cases 2 and 3.

As a result of these parametric sizing studies, case 2 was thought to be optimum because of both the relatively smaller dimmension and higher thermal efficiency. Comparing case 2-1 and case 2-2, the case 2-1 is prefered due to its slimer configuration. Though the primary gas velocity of 19.8 m/s exceeds the assumed allowable value of 15 m/s, this limit is not so serious as explained later in the discussion regarding a self induced vibration. Then, a structural design was carried out specifically for this case.

5. Structural Design

In the above parametric sizing study, the heat duty of IHX was assumed to be 150 MW to ease the comparison among the cases. As case 2-1 has been selected as the optimum one, the same kind of calculation as those conducted in the above parametric study has been repeated for the heat duty of 315 MW. Table 5 shows the results. Among these figures, those regarding the heat transfer and fluid characteristics are as follows:

(a) Number of heat transfer tubes	1,222
(b) Number of coil layers	30
(c) primary He gas pressure drop (including inlet and outlet loss)	0.03 MPa (0.4%)
(d) secondary He gas pressure drop (including inlet and outlet loss)	0.11 MPa (1.4%)
(e) Heat transfer area	3,378 m^2
(f) Coil height	5.75 m
(g) Outer coil diameter	4.05 m
(h) primary He gas velocity	19.5 m/s
(i) secondary He gas velocity	47.6 m/s

It should be pointed out from the comparison between these values with

drop. Since the tube side pressure drop exceeds the allowable limit, an increase in the number of tubes is required in case 1. In case 3 (reactor outlet temperature = 900°C), the heat transfer areas become somewhat smaller compared with case 2 in the outer diameter of ϕ31.8 mm and also ϕ25.4 mm.

Table 4 shows a summary of the parametric sizing study. Here, the values of the heat exchange capacities do not coinside with just 150 MW, because of the convenience of calculation. Though there are some variations due to the limit of the sizing, it can be observed that the dimmensions of case 1 is much larger than those of the other cases in both the number of coil layers and coil height. There is no significant difference in the dimmensions between cases 2 and 3.

As a result of these parametric sizing studies, case 2 was thought to be optimum because of both the relatively smaller dimmension and higher thermal efficiency. Comparing case 2-1 and case 2-2, the case 2-1 is prefered due to its slimer configuration. Though the primary gas velocity of 19.8 m/s exceeds the assumed allowable value of 15 m/s, this limit is not so serious as explained later in the discussion regarding a self induced vibration. Then, a structural design was carried out specifically for this case.

5. Structural Design

In the above parametric sizing study, the heat duty of IHX was assumed to be 150 MW to ease the comparison among the cases. As case 2-1 has been selected as the optimum one, the same kind of calculation as those conducted in the above parametric study has been repeated for the heat duty of 315 MW. Table 5 shows the results. Among these figures, those regarding the heat transfer and fluid characteristics are as follows:

(a) Number of heat transfer tubes	1,222
(b) Number of coil layers	30
(c) primary He gas pressure drop (including inlet and outlet loss)	0.03 MPa (0.4%)
(d) secondary He gas pressure drop (including inlet and outlet loss)	0.11 MPa (1.4%)
(e) Heat transfer area	3,378 m^2
(f) Coil height	5.75 m
(g) Outer coil diameter	4.05 m
(h) primary He gas velocity	19.5 m/s
(i) secondary He gas velocity	47.6 m/s

It should be pointed out from the comparison between these values with

those in Table 4 that the heights of coil are equal in both cases and only the coil diameter increases. This can be understood, if we consider that the heat transfer and fluid parameters such as primary and secondary gas velocities have been kept constant and only the number of tubes were increased to adapt to the increase in the heat duty from 150 MW to 315 MW.

Figure 16 shows the vertical arrangement of IHX. Here, both the vertical and radial pitches are 45 mm. Though the values are 2 mm smaller than those of IHX in HTTR, we have concluded that they could be fabricated.

Inside diameter of the liner of thermal insulation attached to the inside wall of center pipe was determined to be ϕ1,000 mm so that the gas velocity of high temperature secondary outlet He gas is around 40 m/s. When the wall thickness of the liner of 6 mm and the thickness of insulation of 144 mm are selected, the innermost helical coil diameter becomes ϕ1,440 mm. For an inner diameter and a thickness of manifold-type tube header, ϕ900 mm and t40 mm have been selected, respectively. The pitches of tube nozzles on the manifold are 50 mm in the axial direction and 77 mm in the circumferential direction, respectively. The numbers of the nozzles are 31 in the axial direction and 40 in the circumferential direction, respectively. Regarding the outer shell, since the temperature of He gas becomes 560°C, and then, design temperature becomes 590°C, not the 2 1/4Cr-1Mo steel used in the HTTR but Mod.9Cr-1Mo steel with higher strength at the temperature has been adopted.

The integrity of the tubes for the flow induced vibration has been examined. As the shell side gas velocity is the highest at the high temperature section of the helical coil, the tube in this section was selected for examination. Two kinds of vibration mechanisms have been examined.

(a) Vibration caused by eddy generation

In our design, heat transfer promoting plates are provided in the circumferential annuli between the helical coil tube layers. These plates have an additional effect restricting a discharge of eddy from the heat transfer tubes and also a formation of eddy lines. In this type of arrangement, it is assured by the research conducted at the large project of MITI that a flow induced vibration does not occur so long as the ratio of the width of flow channel to the outer diameter of tube is confined within the value defined by the following equation:

$$\frac{H}{d_{\phi}} < 1.53$$

where H = width of flow channel,
d_ϕ = outer diameter of heat transfer tube.

In this case, H=42 mm and d_ϕ=31.8 mm, and then, H/d_ϕ=1.32, which is less than the allowable limit of 1.53. Therefore, it can be concluded that such a kind of vibration will not occur.

(b) Vibration due to a self induced vibration

There is an another kind of vibration. When some numbers of tubes vibrate coincidently, each tube receive mutually energy from the fluid flowing along the surrounding tubes. If this energy is larger than the damping potential of tube, a fluidelastic vibration, which is a kind of the self induced vibration, can occur. The critical velocity for the vibration is given by the following equation:

$$\frac{V_c}{f_n d_\phi} = K\left[\frac{m_e \delta_s}{\rho d_\phi^2}\right]^{0.5}$$

where V_c = critical gas velocity (m/s),
f_n = natural frequency of heat transfer tube (1/s),
d_o = outer diameter of heat transfer tube (m),
m_e = mass of heat transfer tube per unit length (kg/m),
δ_s = logarithmic damping ratio ($=2\pi\zeta$:ζ=0.01)
ρ = density of fluid (kg/m^3).

The term on the left-hand side is called a nondimensional velocity and the term in square bracket on the right-hand side is called a nondimensional damping ratio. The relationship is depicted in Fig. 17. Usually, the critical value is K=10. If a point locates below K=10, it means a stable condition.

In the case of 315 MW IHX, the natural frequecy is calculated by the following equation, which gives a conservative estimation:

$$f_n = \frac{\lambda_n}{2\pi b^2}\left[\frac{EI}{\rho A}\right]^{0.5}$$

where λ_n = nondimensional coefficient depending on supporting condition (in the case of simple support, $\lambda_n=\pi$),
b = length beteen supports (m),
E = linear elastic constant (MPa)
I = secondary cross-sectional moment (m^4),
ρ_t = density of tube material (kg/m^3),

A = cross-sectional area of tube (m^2).

In our case, b=1,367 mm (maximum value), $E=1.28\times10^5$ MPa (the value of Hastelloy XR at 950°C), I=29,800 mm^4, $\rho_t=9.35\times10^{-6}$ kg/mm^3) and A=287.5 mm^2. Therefore, the lowest natural frequency becomes f_n = 31.7 Hz. The shaded area in Fig. 17 shows the data band for the all helical tubes. The maximum value of K, which corresponds to the hottest tube, becomes 3, which is sufficiently less than the critical value. Therefore, such vibration can not be thought to occur.

Consequently, though there remain some uncertainties regarding the fabricability of IHX such as the maximum available size of Ni-Cr-W ingot, precise strength data of Ni-Cr-W superalloy and welding and construction of connecting tubes at the manifold tube header, the IHX of 300 MWt is concluded to be capable of fabrication.

6. Rough Estimate of Dimmensions of IHX in the Other Cases

Coil dimmensions in the other cases can be estimated making use of Table 4.

For example, in case 1, as a heat duty is 455 MW which equals to 152 MW × 3.0, if the heat transfer conditions are not changed, the number of tubes becomes 1,101 multiplied by 3.0 and equals to 3,303. By selecting the nearest number from Table 6, which shows the relation between the number of tubes and that of the coil layers, the number of coil layers of 57 and the number of tubes of 3,349 are selected, where the coil diameter is 6.48m. Regarding the overall dimmensions, if the radial dimmension outside the coil (0.95 m) and the vertical dimmension of the top and bottom plenums (13.95 m) are assumed to be unchanged, the outer diameter becomes 7.43 m, which is the sum of 6.48 m and 0.95 m and also the height becomes 29.4 m which is a sum of 15.45 m and 13.95 m.

By the way, in the above study, the pressure drop in the secondary circuit was limited less than 1.6%. However, if some amount of decrease in the thermal efficiency would be tolerated, a design exceeding the limit could be allowed. Then, the secondary He gas velocity of 29.3m/s is changed to 50 m/s. At this point, a number of tubes can be known to be 655 as seen from Fig. 10. Consequently, it becomes 1,985 for a heat duty of 455 MW. Under this condition, the number of coil layers and outside diameter of the coil become 41 and 5.04 m, respectively. The secondary pressure drop can be seen as 3.75% from Fig. 15.

A = cross-sectional area of tube (m^2).

In our case, b=1,367 mm (maximum value), $E=1.28\times10^5$ MPa (the value of Hastelloy XR at 950°C), I=29,800 mm^4, $\rho_t=9.35\times10^{-6}$ kg/mm^3) and A=287.5 mm^2. Therefore, the lowest natural frequency becomes f_n = 31.7 Hz. The shaded area in Fig. 17 shows the data band for the all helical tubes. The maximum value of K, which corresponds to the hottest tube, becomes 3, which is sufficiently less than the critical value. Therefore, such vibration can not be thought to occur.

Consequently, though there remain some uncertainties regarding the fabricability of IHX such as the maximum available size of Ni-Cr-W ingot, precise strength data of Ni-Cr-W superalloy and welding and construction of connecting tubes at the manifold tube header, the IHX of 300 MWt is concluded to be capable of fabrication.

6. Rough Estimate of Dimmensions of IHX in the Other Cases

Coil dimmensions in the other cases can be estimated making use of Table 4.

For example, in case 1, as a heat duty is 455 MW which equals to 152 MW × 3.0, if the heat transfer conditions are not changed, the number of tubes becomes 1,101 multiplied by 3.0 and equals to 3,303. By selecting the nearest number from Table 6, which shows the relation between the number of tubes and that of the coil layers, the number of coil layers of 57 and the number of tubes of 3,349 are selected, where the coil diameter is 6.48m. Regarding the overall dimmensions, if the radial dimmension outside the coil (0.95 m) and the vertical dimmension of the top and bottom plenums (13.95 m) are assumed to be unchanged, the outer diameter becomes 7.43 m, which is the sum of 6.48 m and 0.95 m and also the height becomes 29.4 m which is a sum of 15.45 m and 13.95 m.

By the way, in the above study, the pressure drop in the secondary circuit was limited less than 1.6%. However, if some amount of decrease in the thermal efficiency would be tolerated, a design exceeding the limit could be allowed. Then, the secondary He gas velocity of 29.3m/s is changed to 50 m/s. At this point, a number of tubes can be known to be 655 as seen from Fig. 10. Consequently, it becomes 1,985 for a heat duty of 455 MW. Under this condition, the number of coil layers and outside diameter of the coil become 41 and 5.04 m, respectively. The secondary pressure drop can be seen as 3.75% from Fig. 15.

As a second example, it is discussed to decrease the dimmensions by reducing the heat transfer area as a result of increase in the logarithmic mean temperature difference. When the logarithmic mean temperature difference is multiplied by 1.5, that is, 60°C, the heat transfer area can be reduced to 2/3. Here, the effects of changes in the inlet or outlet temperature and pressure on the overall heat transfer coefficient are small as explained in Section 4.3, and then, they are neglected in the present discussion. As it is desirable to decrease the diameter rather than the length, the upper limit value of 50 m/s for the secondary gas velocity is selected. Here, the total number of tubes are 655. The coil height in this condition can be obtained in Fig. 14 as an intersection between the line reducing the value of case 1 to 2/3 and a vertical line of 655, which is 1.87%. As the number of tubes for 455 MW is 1.985 as shown in the former example, the total dimmensions become ϕ6.0 m × H26.8 m. Similarly, when the logarithmic mean temperature difference is magnified to twice (80°C) and twice and a half (100°C), the coil height is reduced to 9.6 and 7.7 m and also the secondary pressure drop decreases to 1.9 and 1.5%, respectively.

Here, we examine how adversely thermal cycle efficiency is affected by the increase of the logarithmic mean temperature difference. Using the above pressure drop ratio, the cycle calculations give the results shown in Fig. 18. The reason why the thermal cycle efficiency decreases in accordance with the increase in the logarithmic mean temperature difference is because a smaller pressure ratio is required owing to a reduction in the compressor outlet temperature.

It was clarified that the logarithmic mean temperature difference of 40°C given as the initial assumption was too small to obtain a reasonable size of IHX. However, it is not simple to decide an optimum value for it. That will be determined by a comprehensive study on the trade off between many factors such as heat duty, fabrication capability, cost and thermal cycle efficiency.

Then, we consider to reduce the logarithmic mean temperature difference of 129°C for case 2. We will change the coil height only while the number of tubes is kept constant, that is, the outer coil diameter is kept constant. In accordance with the decrease in the logarithmic mean temperature difference stepwise like 100, 80 and 60°C, it is known that the coil height increases to 7.42 m, 9.27 m and 12.36 m, and then, the secondary pressure loss increases to 2.1, 2.6 and 3.4%. However, in cases 2 and 3, the thermal cycle efficiency does not increase even if the logarithmic mean temperature difference are reduced because in both cases, a temperature difference at the pinch point and also that between the gas turbine outlet temperature and

the steam temperature(540°C) confine the pressure ratio in the gas turbine cycle. However, in the case of another steam pressure or a steam cycle with a steam extraction, a thermal cycle efficiency is affected by a logarithmic mean temperature difference.

Though the temperature conditions are different, the predictions of characteristics in the case coupled with a reheat steam extraction cycle at the steam pressure of 14 MPa are shown in Fig. 19. In this example, at the logarithmic mean temperature difference of 73°C, a temperature difference between the gas turbine outlet temperature and the steam temperature reaches the allowable limit of 40°C. On the other hand, the temperature difference between the He gas temperature of the precooler cold leg and the temperature of feed water reaches the allowable limit of 20°C at 109°C. Therefore, the permissible values for the logarithmic mean temperature difference is confined within a small range. Nevertheless, the value of 100°C is known to be optimum.

7. Summary and Conclusions

High thermal efficiency can be achieved in a power generation system, which couples a high temperature gas-cooled reactor(HTGR) with a closed cycle gas turbine(GT). There are three possible systems such as a direct cycle (DC), an indirect cycle (IDC) and an indirect gas-steam combined cycle (IDCC). An intermediate heat exchanger(IHX) is needed in IDC or IDCC. The size of IHX is claimed to become too large to allow a reasonable design and it becomes one of the most important issues. Then, a design has been carried out based on the experience of IHX in HTTR.

Cycle calculations have been carried out for the three cases. The first case is IDCC of a perfect cascade type. The second and third cases are of the semi-cascade type. The reactor outlet temperature is 950°C for both cases 1 and 2. On the other hand, that of case 3 is 900°C. The pressure of both the primary and secondary circuits are about 8 MPa. The thermal cycle efficiencies in cases 1 and 2 are about 47%. That in case 3 is 45.5%.

As the material of high temperature components, a Ni-Cr-W superalloy with the highest strength at temperature was adopted instead of Hastelloy XR used in HTTR. The values of maximum allowable stress intensity denoted So have been prepared based on the experimental creep-rupture strength. The outer diameter and thickness of heat transfer tubes have been determined so as to meet the stress limits for both the design pressure and design load, which is a dead weight load at the connecting tube between the helical tube and the tube header.

the steam temperature(540°C) confine the pressure ratio in the gas turbine cycle. However, in the case of another steam pressure or a steam cycle with a steam extraction, a thermal cycle efficiency is affected by a logarithmic mean temperature difference.

Though the temperature conditions are different, the predictions of characteristics in the case coupled with a reheat steam extraction cycle at the steam pressure of 14 MPa are shown in Fig. 19. In this example, at the logarithmic mean temperature difference of 73°C, a temperature difference between the gas turbine outlet temperature and the steam temperature reaches the allowable limit of 40°C. On the other hand, the temperature difference between the He gas temperature of the precooler cold leg and the temperature of feed water reaches the allowable limit of 20°C at 109°C. Therefore, the permissible values for the logarithmic mean temperature difference is confined within a small range. Nevertheless, the value of 100°C is known to be optimum.

7. Summary and Conclusions

High thermal efficiency can be achieved in a power generation system, which couples a high temperature gas-cooled reactor(HTGR) with a closed cycle gas turbine(GT). There are three possible systems such as a direct cycle (DC), an indirect cycle (IDC) and an indirect gas-steam combined cycle (IDCC). An intermediate heat exchanger(IHX) is needed in IDC or IDCC. The size of IHX is claimed to become too large to allow a reasonable design and it becomes one of the most important issues. Then, a design has been carried out based on the experience of IHX in HTTR.

Cycle calculations have been carried out for the three cases. The first case is IDCC of a perfect cascade type. The second and third cases are of the semi-cascade type. The reactor outlet temperature is 950°C for both cases 1 and 2. On the other hand, that of case 3 is 900°C. The pressure of both the primary and secondary circuits are about 8 MPa. The thermal cycle efficiencies in cases 1 and 2 are about 47%. That in case 3 is 45.5%.

As the material of high temperature components, a Ni-Cr-W superalloy with the highest strength at temperature was adopted instead of Hastelloy XR used in HTTR. The values of maximum allowable stress intensity denoted So have been prepared based on the experimental creep-rupture strength. The outer diameter and thickness of heat transfer tubes have been determined so as to meet the stress limits for both the design pressure and design load, which is a dead weight load at the connecting tube between the helical tube and the tube header.

Parametric design studies have been undertaken for the common value of a heat duty of 150 MW. Heat transfer characteristics such as the shell side and tube side gas velocities, an overall heat transfer coefficient, a heat transfer area and a helical coil height have been clarified on the dependence of the number of tubes. Then, pressure drops both in the shell and tube sides were calculated. Consequently, the design points regarding the number of tubes and associated design parameters have been determined to meet the assumed design limits. As the optimum case, case 2 was selected because of both its smaller size and high thermal cycle efficiency.

Then, IHX of 315 MW has been designed specifically and its dimensions and structures were determined. In addition, a flow induced vibration of tubes were examined regarding the assumed limit for the shell side gas velocity. IHX was clarified to be capable of fabrication at least in the case of the semi-cascade type in IDCC.

The results of the parametric studies are useful to make a rough estimate for the other cases and some examples are shown.

Acknowledgments

The authors would like to express their thanks to Dr.H.Tsuji for his kind cooperation regarding the data of Ni-Cr-W superalloy.

Parametric design studies have been undertaken for the common value of a heat duty of 150 MW. Heat transfer characteristics such as the shell side and tube side gas velocities, an overall heat transfer coefficient, a heat transfer area and a helical coil height have been clarified on the dependence of the number of tubes. Then, pressure drops both in the shell and tube sides were calculated. Consequently, the design points regarding the number of tubes and associated design parameters have been determined to meet the assumed design limits. As the optimum case, case 2 was selected because of both its smaller size and high thermal cycle efficiency.

Then, IHX of 315 MW has been designed specifically and its dimensions and structures were determined. In addition, a flow induced vibration of tubes were examined regarding the assumed limit for the shell side gas velocity. IHX was clarified to be capable of fabrication at least in the case of the semi-cascade type in IDCC.

The results of the parametric studies are useful to make a rough estimate for the other cases and some examples are shown.

Acknowledgments

The authors would like to express their thanks to Dr.H.Tsuji for his kind cooperation regarding the data of Ni-Cr-W superalloy.

References

[1] GCRA: Evaluation of the gas turbine modular helium reactor, DOE-HTGR-90380 Final Draft (Dec. 1993).
[2] Muto,Y.:"Thermal Cycle Efficiency of the Indirect Combined HTGR-GT Power Generation System", JAERI-Tech 96-006 (Feb. 1996).
[3] Saito,S.: International Conference on Design and Safety of Advanced Nuclear Power Plants, pp.7.1-1, Tokyo, Oct. 25-29 (1992).
[4] Tsuji,H., Nakajima,H. and Kondo,T.:"Development of a New Ni-Cr-W Superalloy for Application to High Temperature Structures", Proceedings of International Conference on Materials for Advanced Power Engineering, Kluwer Academic Publishers, pp.939-948 (1994).
[5] Hada,K.:"Development of metallic materials and a high-temperature structural design code for the HTTR", Nuclear Engineering and Design, Vol.132, pp.1-11 (1991).
[6] Blass,J.J., Corum,J.M. and Chang,S.-J.:"Methods for Very High Temperature Design", Proceedings of the Workshop on Structural Design Criteria for HTR, Jül-Conf-71, pp.206-227 (April 1989).
[7] Tsuji,H.: Private communication (1993).
[8] Haynes International, Inc.: "HAYNES Alloy No.230", products catalogue (1991).
[9] Lidsky,L.M. and Yan,X.: Proceedings of International Conference on Design and Safety of Advanced Nuclear Power Plants, pp.8.1-1, Tokyo, Oct. 25-29 (1992).

Table 1. Design conditions for the IHX

Items		Case 1	Case 2	Case 3
Heat duty	MW	456	315	311
1ry He gas				
Inlet pressure	MPa	7.7	7.7	7.7
Inlet temperature	℃	950	950	900
Outlet temperature	℃	389	562	551
Flow rate	kg/s	156 (51.5)	156 (74.4)	172 (82.8)
2ry He gas				
Inlet pressure	MPa	7.9	7.9	7.9
Inlet temperature	℃	350	255	223
Outlet temperature	℃	910	910	850
Flow rate	kg/s	156 (51.6)	92.7 (44.1)	95.6 (46.1)
Logarithmic mean temperature difference	℃	40	131	148
Thermal cycle efficiency	%	47.4	47.2	45.5

Note : Figures in parenthesis show those for the heat exchange capacity of 150 MW.

Table 2. Maximum allowable stress intensity So for the Ni-Cr-W superalloy

Temperature °C	Experimental average creep-rupture strength MPa	90% of the left MPa	2/3 of the left = So MPa
600	190.49	171.44	114.3
650	138.80	124.92	83.3
700	100.04	90.03	60.0
750	71.24	64.11	42.7
800	50.05	45.04	30.0
850	34.63	31.16	20.8
900	23.54	21.19	14.1
950	15.69	14.12	9.4
1000	10.21	9.19	6.1

Table 3. Thermal conductivity for the Tungsten alloy[8]

Temperature °C	Thermal conductivity W/m°K	Temperature °C	Thermal conductivity W/m°K
R.T.	8.9	600	20.4
100	10.4	700	22.4
200	12.4	800	24.4
300	14.4	900	26.4
400	16.4	1000	28.4
500	18.4		

Table 4. Results of parametric sizing study

Items		Case 1-1	Case 2-1	Case 2-2	Case 3A-1	Case 3A-2	Case 3B-1
Heat exchange capacity	MW	152	158	158	156	156	156
Thermal cycle efficiency	%	47.4	47.2	47.2	45.5	45.5	45.5
Number of tubes		1,101	600	834	558	834	973
Number of coils		30	20	25	19	25	27
1ry He-gas velocity	m/s	7.2	19.8	14.3	22.5	15.0	13.9
2ry He-gas velocity	m/s	29.3	48.4	34.8	47.4	31.7	47.1
1ry side pressure drop	kPa	8.9	22.8	11.1	26.1	10.9	8.5
2ry side pressure drop	kPa	89.1	99.5	49.5	85.9	37.0	94.4
Heat transfer area	m^2	8,172	1,659	2,016	1,354	1,733	1,451
Outer diameter of coil	m	3.78	2.88	3.33	2.79	3.33	3.20
Helical coil height	m	15.45	5.75	5.03	5.05	4.32	3.88

Note : Case No.-1 denotes sizing based on 2ry pressure drop limit(100kPa).
Case No.-2 denotes sizing based on 1ry He-gas velocity(15m/s).
Case 3A denotes ϕ 31.8mm.
Case 3B denotes ϕ 25.4mm.

Table 5. Specifications of 315 MW IHX

Type		Helical coil, counter flow type
Heat exchange capacity	MW	315
Shell side Fluid		1ry He-gas
Flow rate	kg/s	156.2
Inlet/outlet temperature	℃	950 / 562
Inlet/outlet pressure	MPa	7.60 / 7.57
Tube side Fluid		2ry He-gas
Flow rate	kg/s	92.7
Inlet/outlet temperature	℃	255 / 910
Inlet/outlet pressure	MPa	7.81 / 7.70
Heat transfer area	m^2	3,378
Heat transfer tube		
Material		Ni-Cr-W alloy
Outside diameter	m	31.8
Thickness	m	3.2
Number		1,222
Effective length	mm	27,670
Helical coil		
Number of layers		30
Outside diameter	mm	4,050
Inside diameter	mm	1,440
Effective height	mm	5,750
Pitch(axial/radial)	mm	45/45
Thermal insulation		Alumina-Silica Fibers
Outer shell		
Material		Mod.9Cr-1Mo steel
Outer diameter(Upper/lower)	mm	5,270 / 5,000
Height	m	~19.5

Table 6. Relationship between the number of tubes and the number of layers in the helical coil

Average inclined angle of tubes = 12.0 degrees,
Radial pitch = 45.0mm,
Axial pitch = 45.0mm,
Minimum coil diameter = 1440.0mm.

Number of layers	Total number of tubes	Number of tubes per layer	Helical coil diameter, mm	Inclined angle, deg.
1	21	21	1440.0	11.951
2	44	23	1530.0	12.318
3	68	24	1620.0	12.140
4	93	25	1710.0	11.981
5	120	27	1800.0	12.291
6	148	28	1890.0	12.140
7	177	29	1980.0	12.003
8	208	31	2070.0	12.272
9	240	32	2160.0	12.140
10	273	33	2250.0	12.019
11	308	35	2340.0	12.256
12	344	36	2430.0	12.140
13	381	37	2520.0	12.032
14	420	39	2610.0	12.244
15	460	40	2700.0	12.140
16	502	42	2790.0	12.335
17	544	42	2880.0	11.951
18	588	44	2970.0	12.140
19	634	46	3060.0	12.318
20	681	47	3150.0	12.227
21	729	48	3240.0	12.140
22	778	49	3330.0	12.058
23	829	51	3420.0	12.220
24	881	52	3510.0	12.140
25	934	53	3600.0	12.064

Table 6. Relationship between the number of tubes and the number of layers in the helical coil (continued)

Average inclined angle of tubes = 12.0 degrees,
Radial pitch = 45.0mm,
Axial pitch = 45.0mm,
Minimum coil diameter = 1440.0mm.

Number of layers	Total number of tubes	Number of tubes per layer	Helical coil diameter mm	Inclined angle deg.
26	989	55	3690.0	12.214
27	1045	56	3780.0	12.140
28	1103	58	3870.0	12.281
29	1161	58	3960.0	12.003
30	1222	61	4050.0	12.342
31	1283	61	4140.0	12.074
32	1346	63	4230.0	12.204
33	1410	64	4320.0	12.140
34	1475	65	4410.0	12.078
35	1542	67	4500.0	12.201
36	1610	68	4590.0	12.140
37	1680	70	4680.0	12.256
38	1750	70	4770.0	12.026
39	1823	73	4860.0	12.308
40	1896	73	4950.0	12.085
41	1971	75	5040.0	12.194
42	2047	76	5130.0	12.140
43	2124	77	5220.0	12.088
44	2203	79	5310.0	12.191
45	2283	80	5400.0	12.140
46	2365	82	5490.0	12.239
47	2448	83	5580.0	12.189
48	2532	84	5670.0	12.140
49	2617	85	5760.0	12.093
50	2704	87	5850.0	12.187

Table 6. Relationship between the number of tubes and the number of layers in the helical coil (continued)

Average inclined angle of tubes = 12.0 degrees,
Radial pitch = 45.0mm,
Axial pitch = 45.0mm,
Minimum coil diameter = 1440.0mm.

Number of layers	Total number of tubes	Number of tubes per layer	Helical coil diameter mm	Inclined angle deg.
51	2792	88	5940.0	12.140
52	2882	90	6030.0	12.230
53	2972	90	6120.0	12.051
54	3065	93	6210.0	12.272
55	3158	93	6300.0	12.097
56	3253	95	6390.0	12.183
57	3349	96	6480.0	12.140
58	3447	98	6570.0	12.223
59	3545	98	6660.0	12.058
60	3646	101	6750.0	12.261
61	3747	101	6840.0	12.100
62	3850	103	6930.0	12.179
63	3954	104	7020.0	12.140
64	4060	106	7110.0	12.217
65	4166	106	7200.0	12.064
66	4275	109	7290.0	12.252
67	4384	109	7380.0	12.103
68	4495	111	7470.0	12.177
69	4607	112	7560.0	12.140
70	4721	114	7650.0	12.211
71	4835	114	7740.0	12.070
72	4952	117	7830.0	12.244
73	5069	117	7920.0	12.106
74	5188	119	8010.0	12.174
75	5308	120	8100.0	12.140

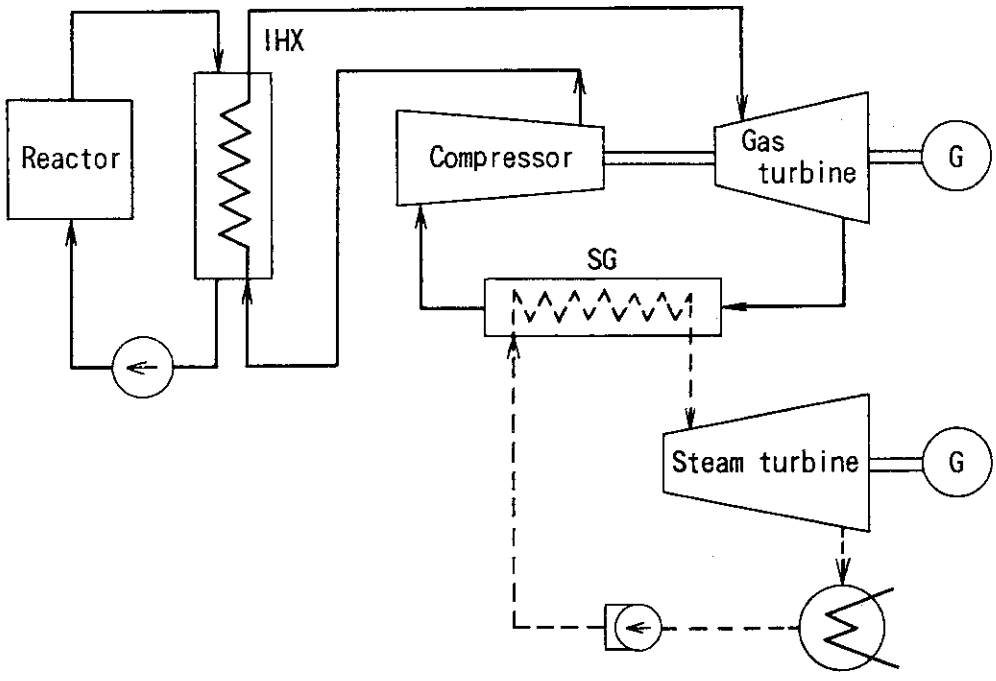

(a) Perfect Cascade Type

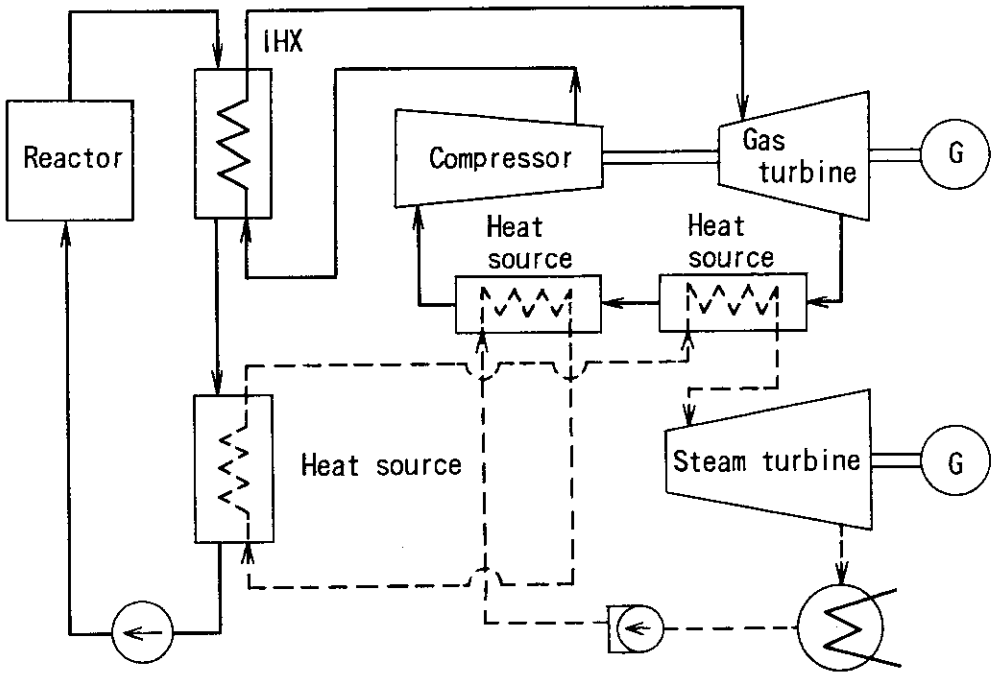

(b) Semi-Cascade Type

Fig. 1. Two flow schemes of indirect combined cycle.

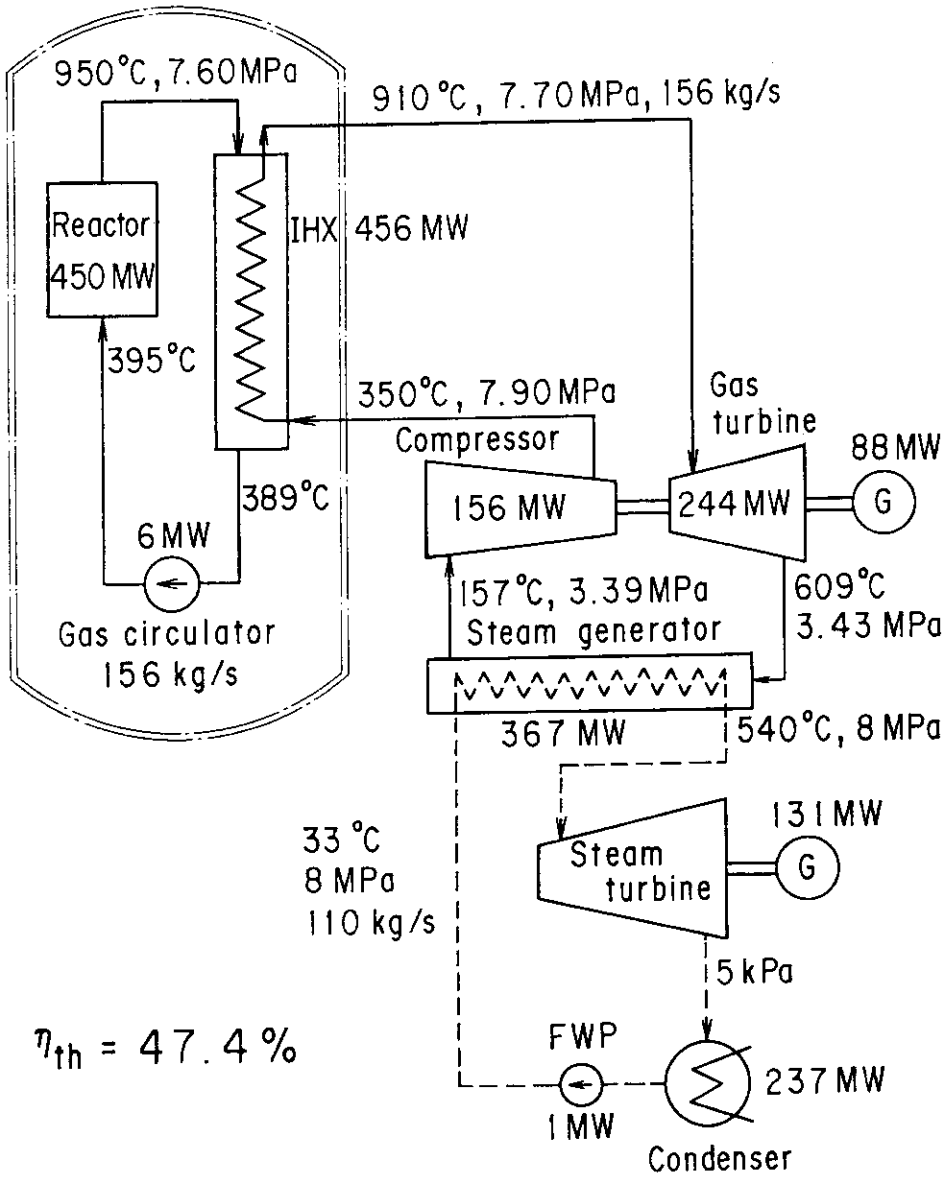

Fig. 2. Flow and heat balance for Case 1.

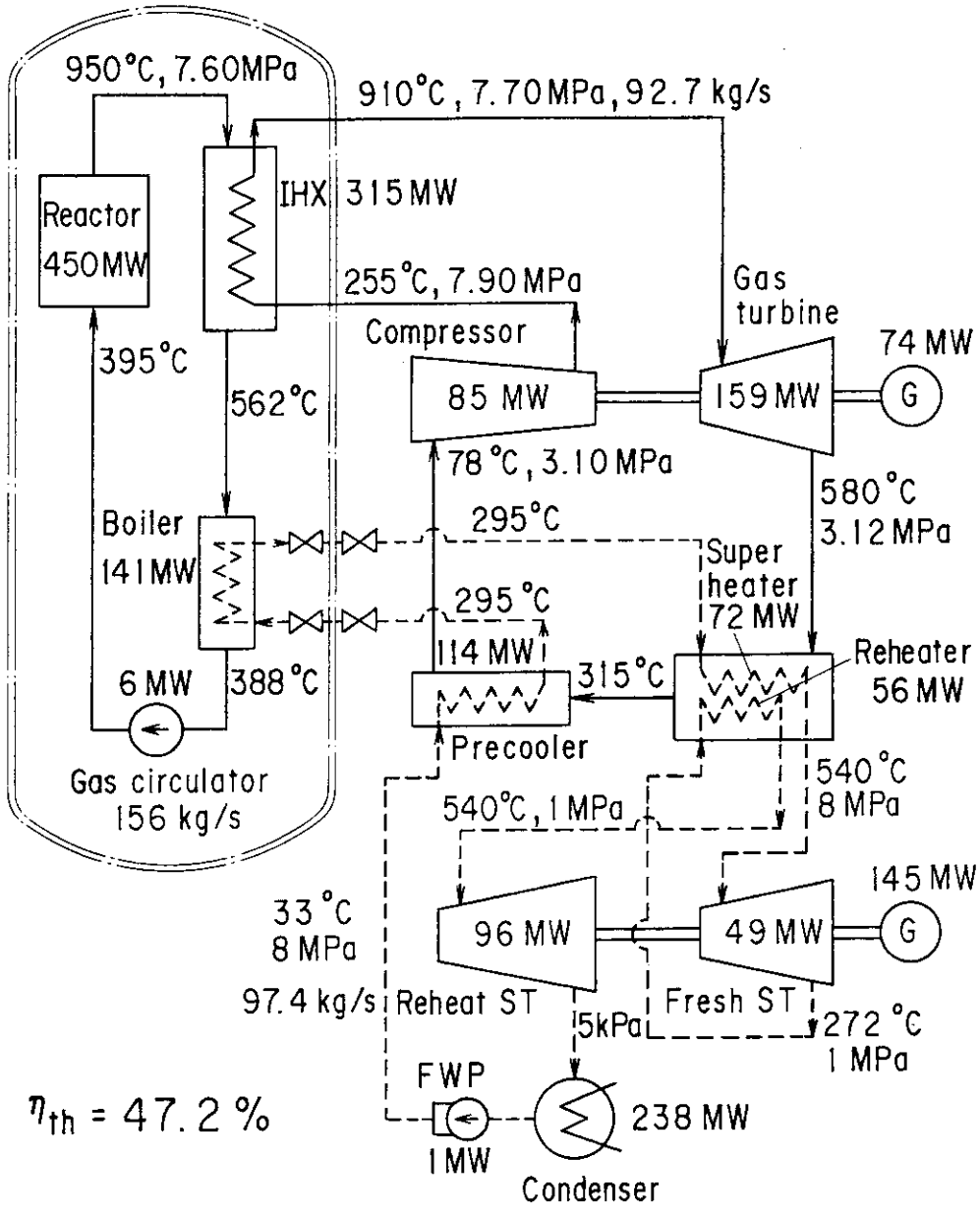

Fig. 3. Flow and heat balance for Case 2.

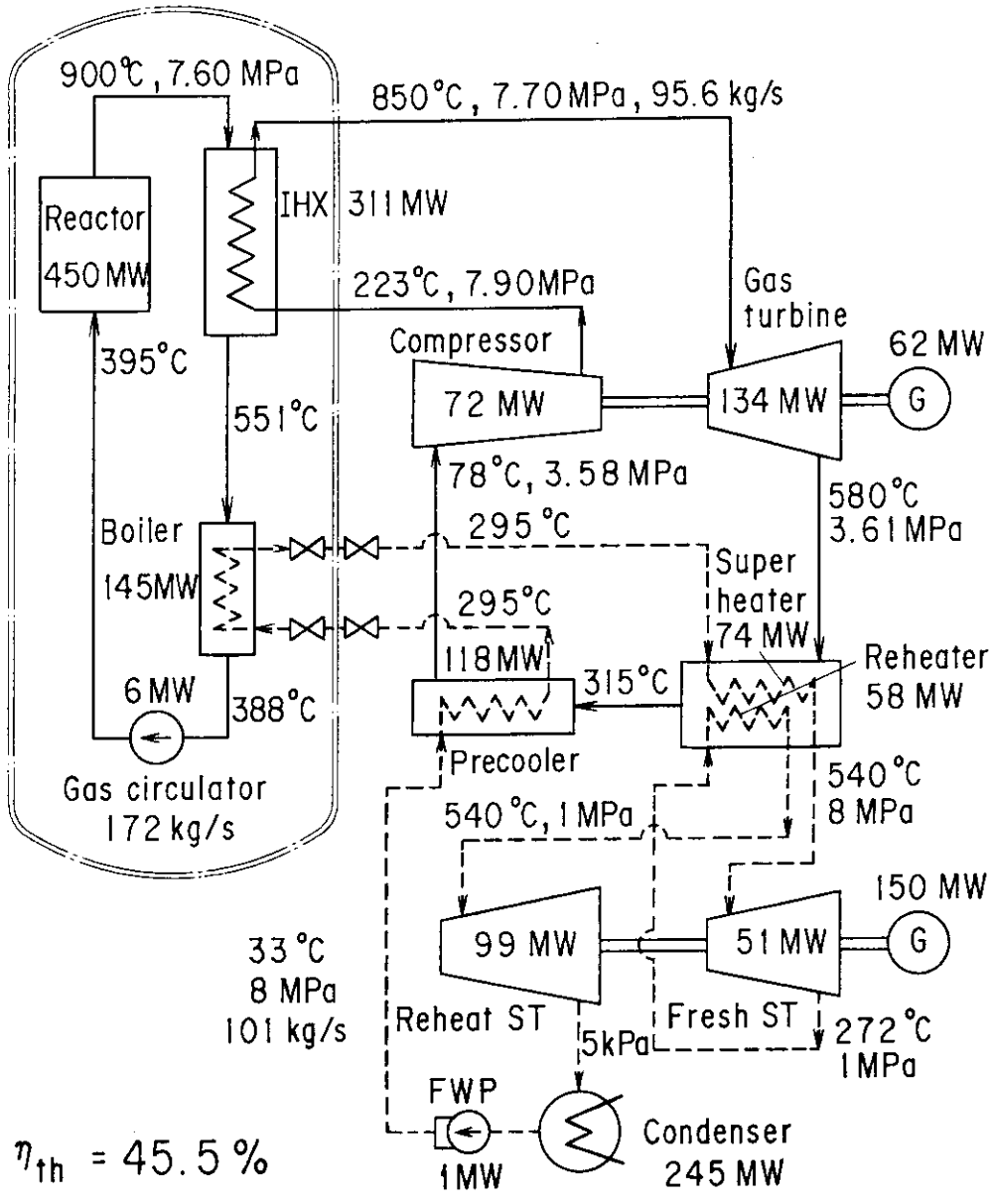

Fig. 4. Flow and heat balance for Case 3.

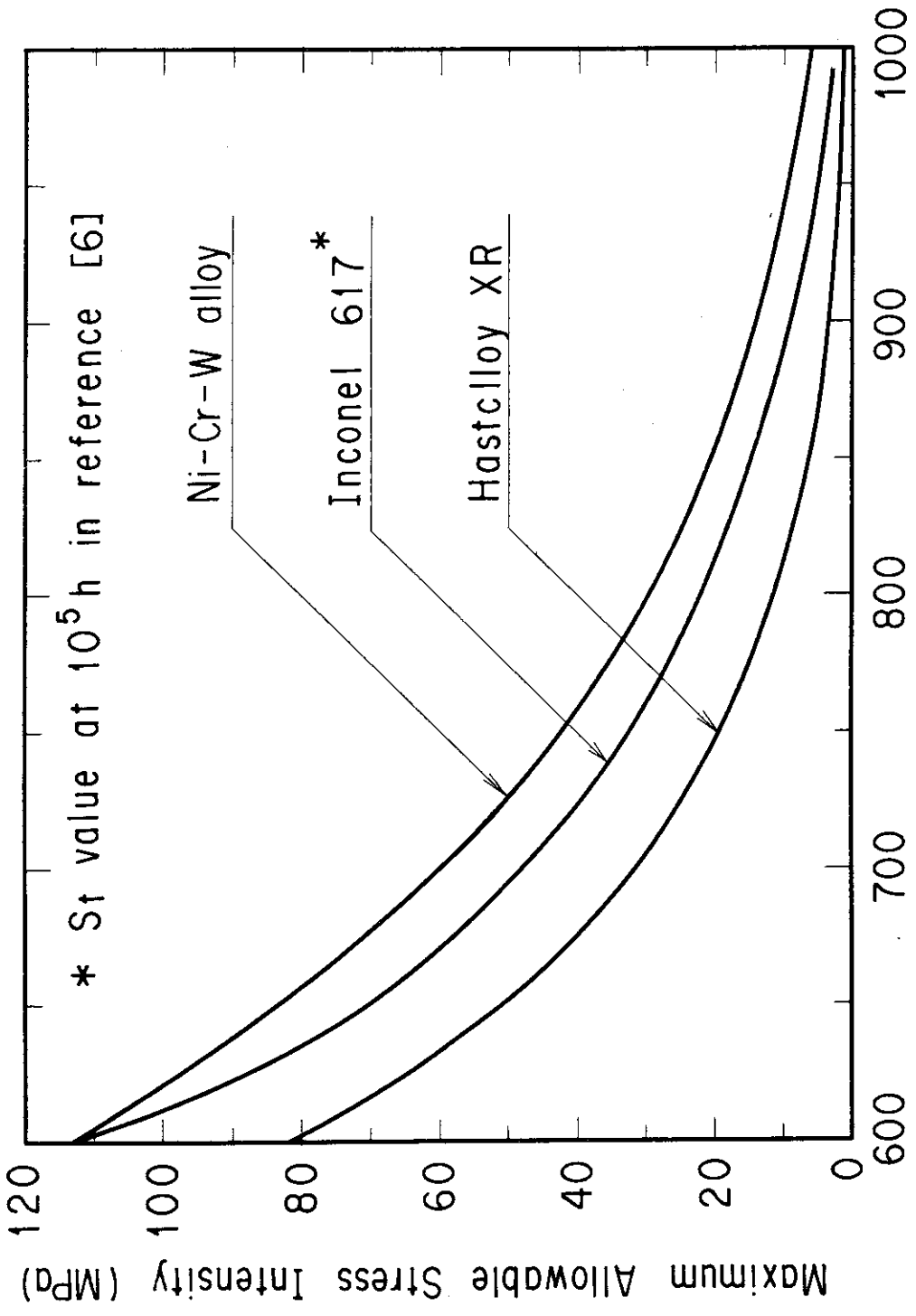

Fig. 5. Maximum allowable stress intensity So for the Ni-Cr-W superalloy, Hastelloy XR and Inconel 617.

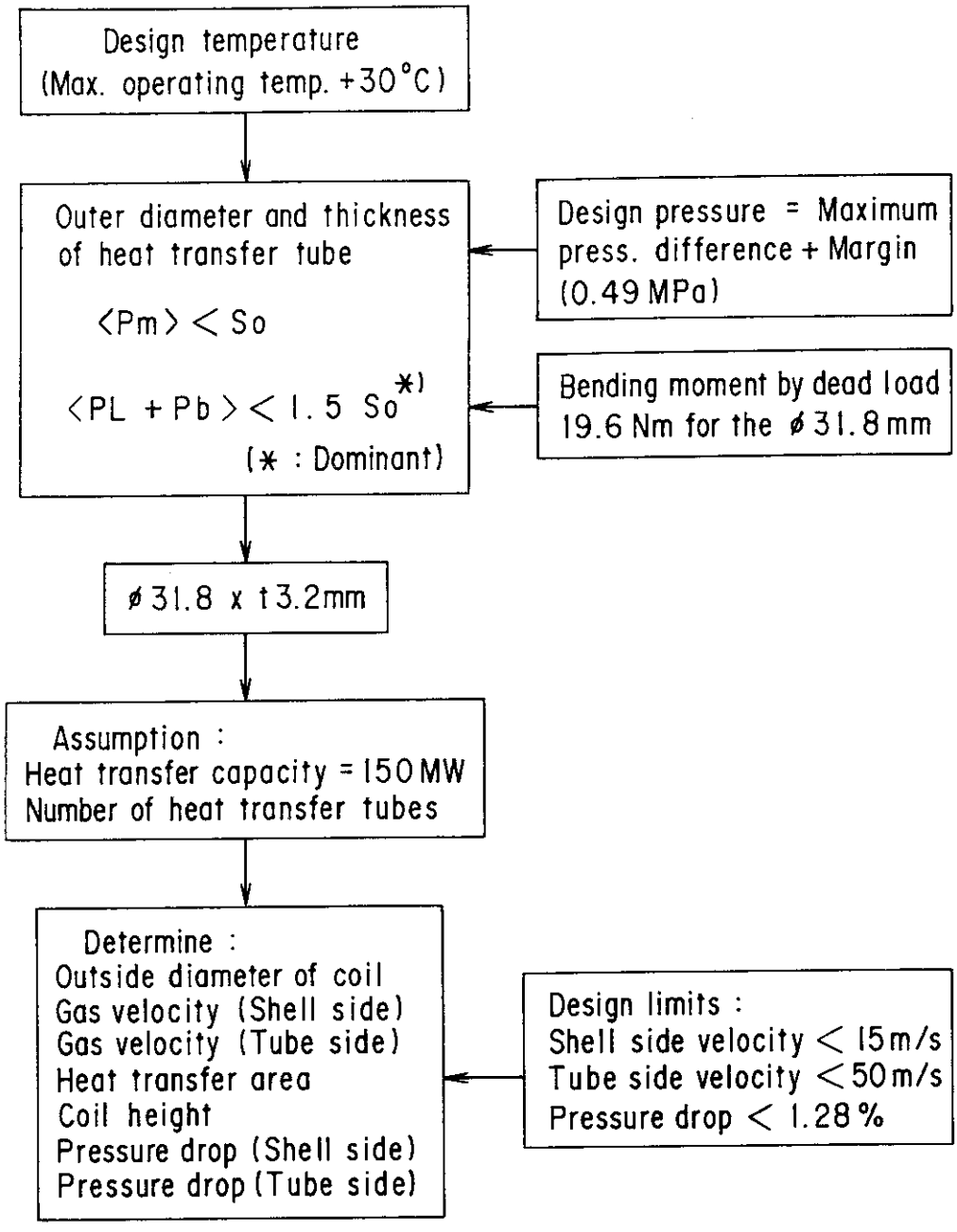

Fig. 6. Sizing procedure for IHX.

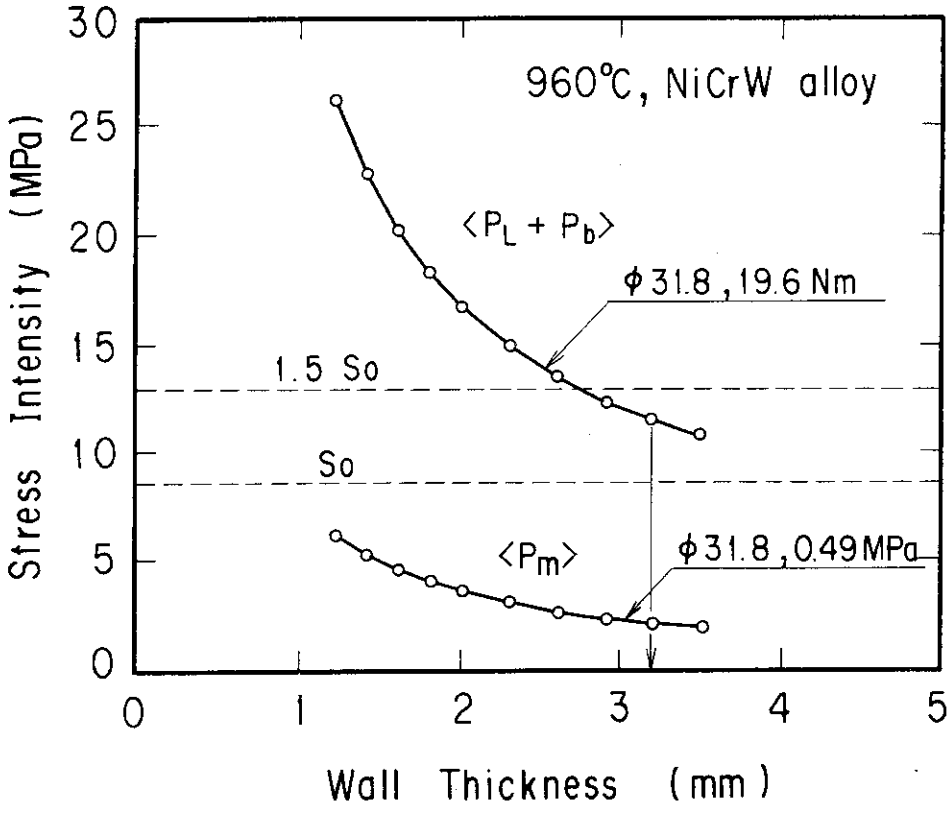

Fig. 7. Stress intensities limits at 960°C in Cases 1 and 2.

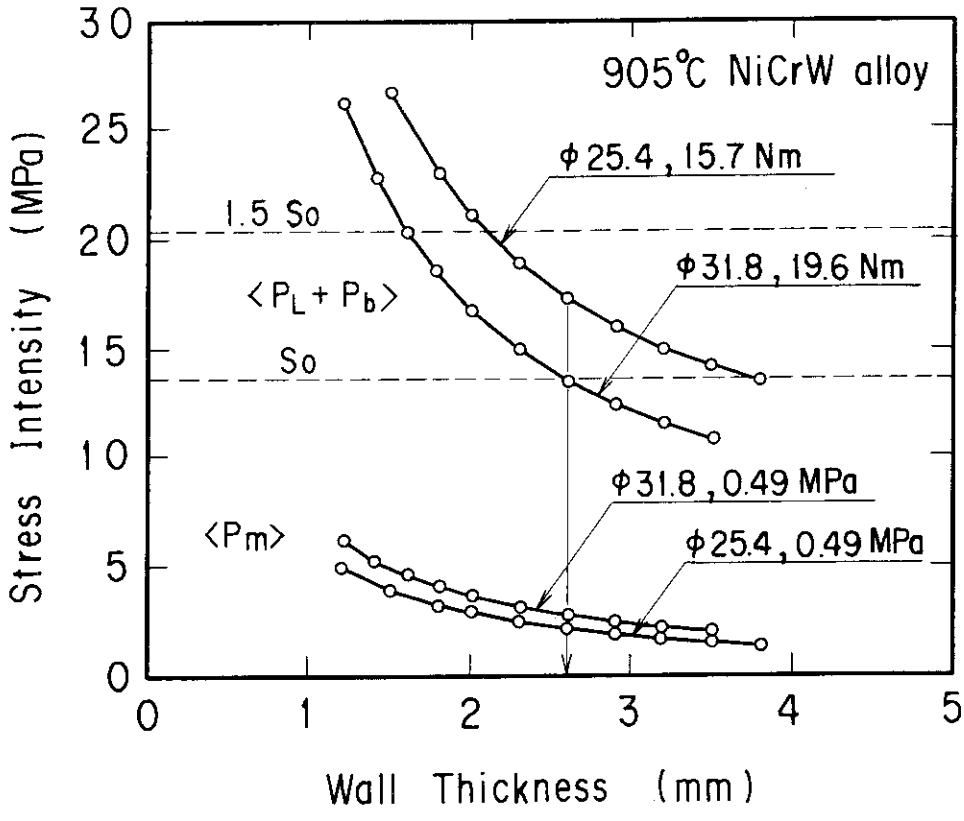

Fig. 8. Stress intensities limits at 905°C in Case 3.

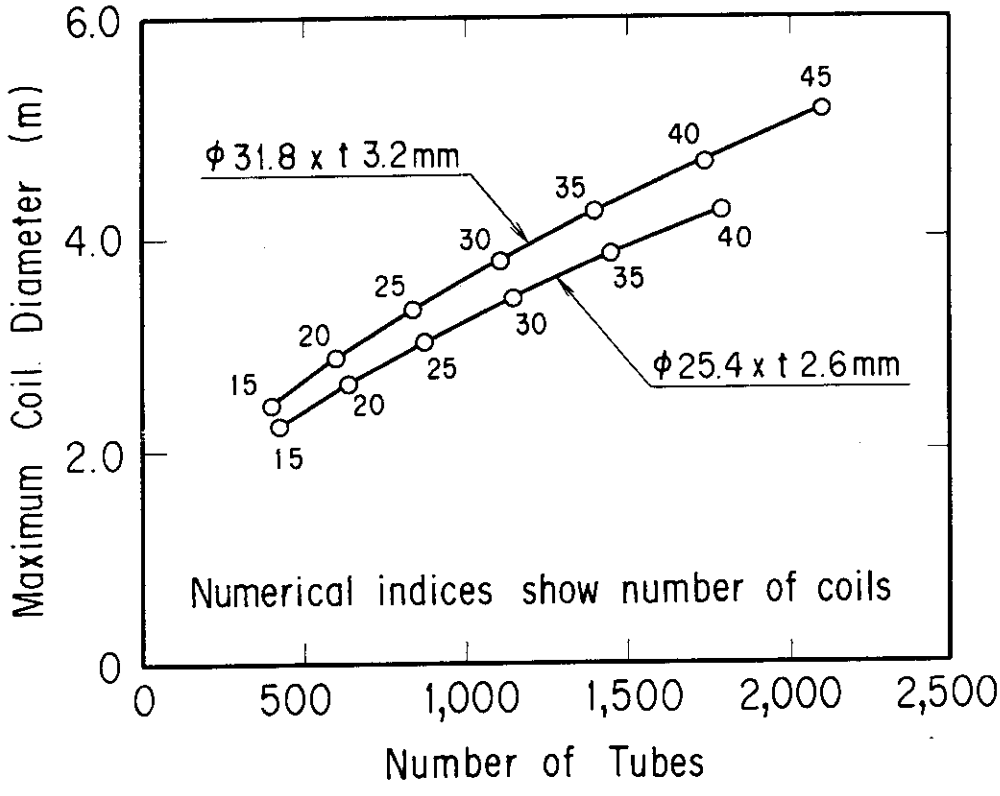

Fig. 9. Maximum coil diameter versus number of tubes.

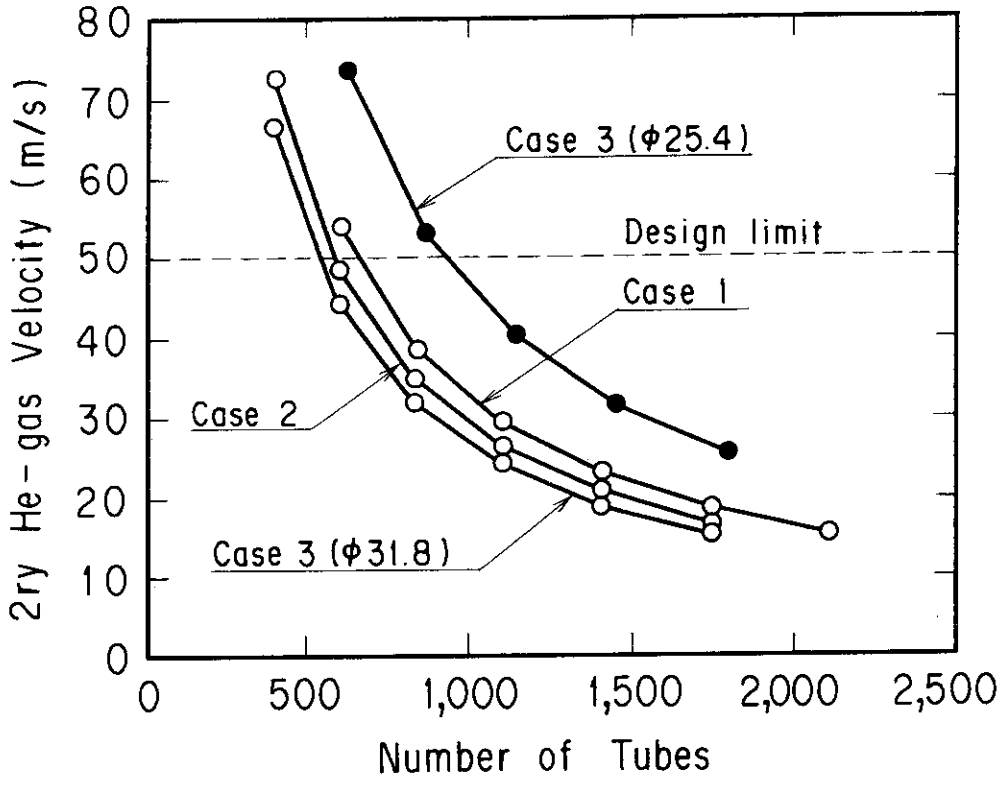

Fig.10. Secondary helium gas velocity versus number of tubes.

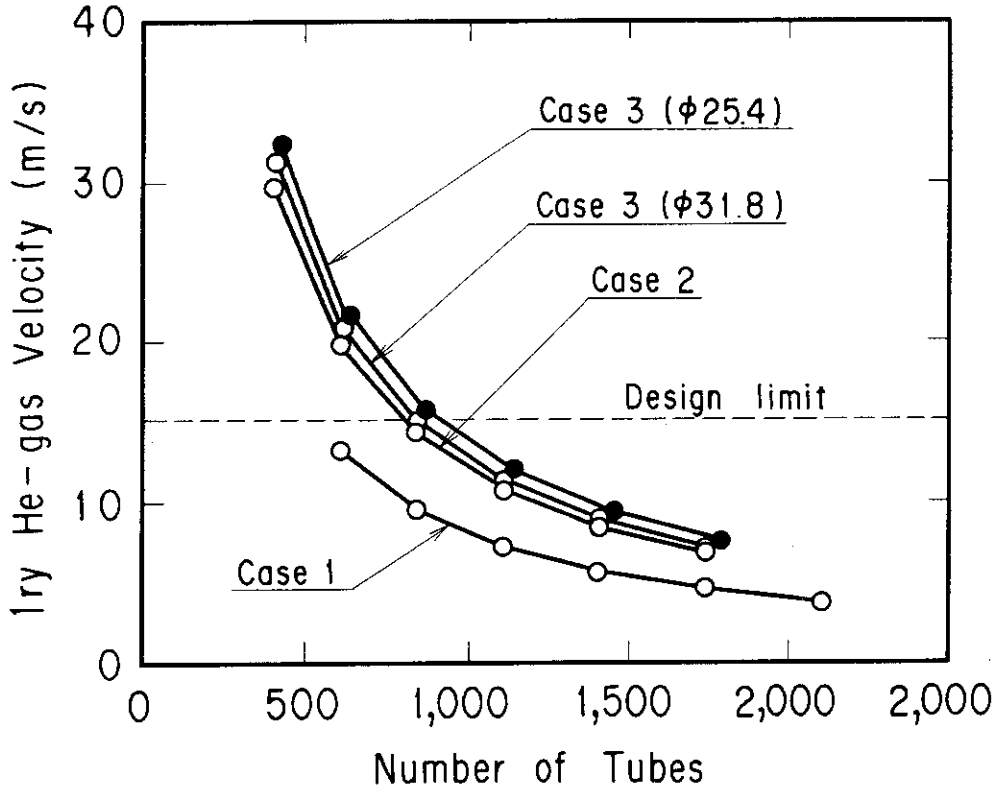

Fig.11. Primary helium gas velocity versus number of tubes.

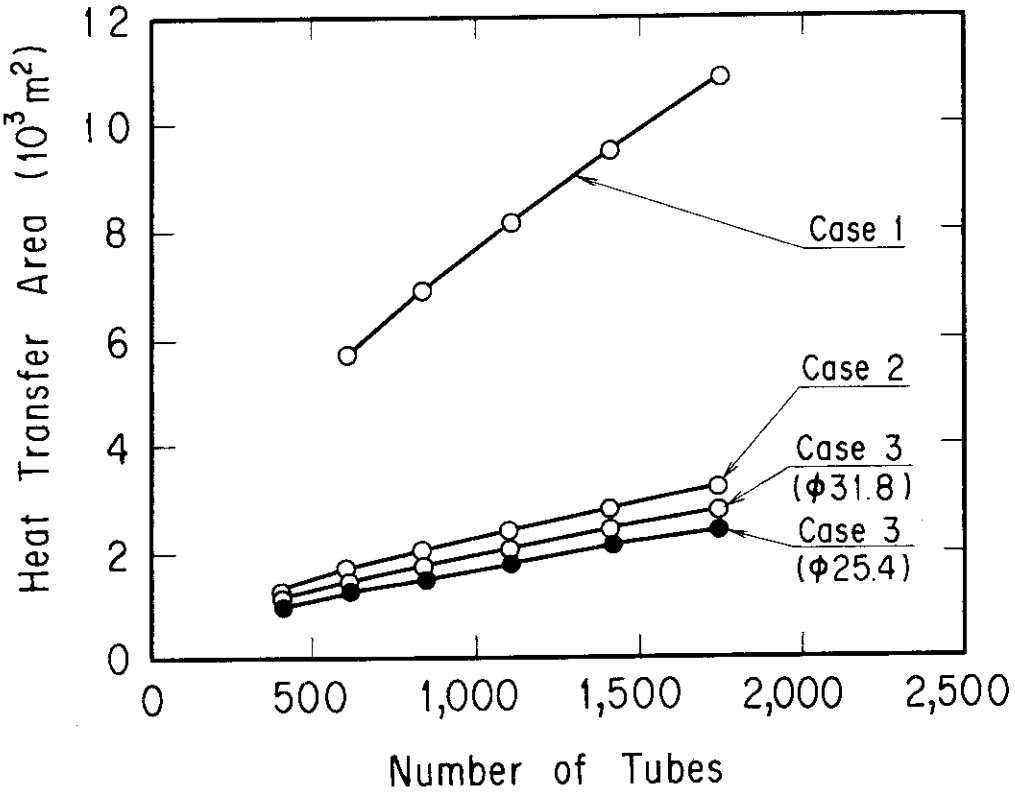

Fig.12. Required heat transfer area dependent on number of tubes.

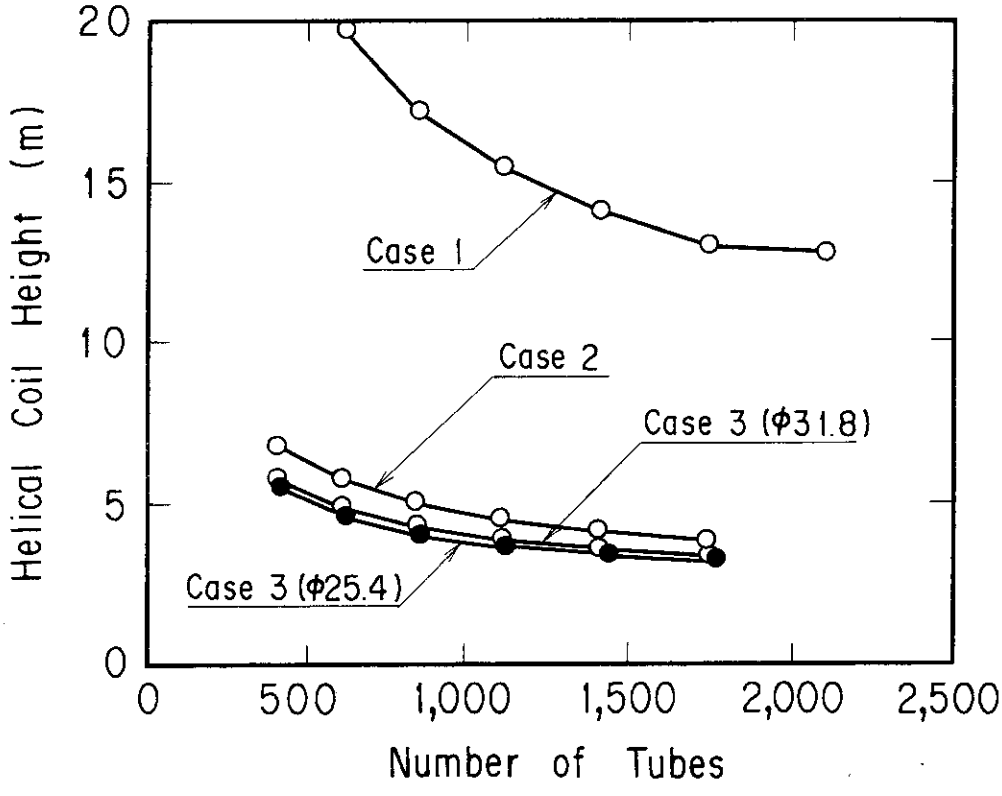

Fig.13. Dependence of helical coil height on number of tubes.

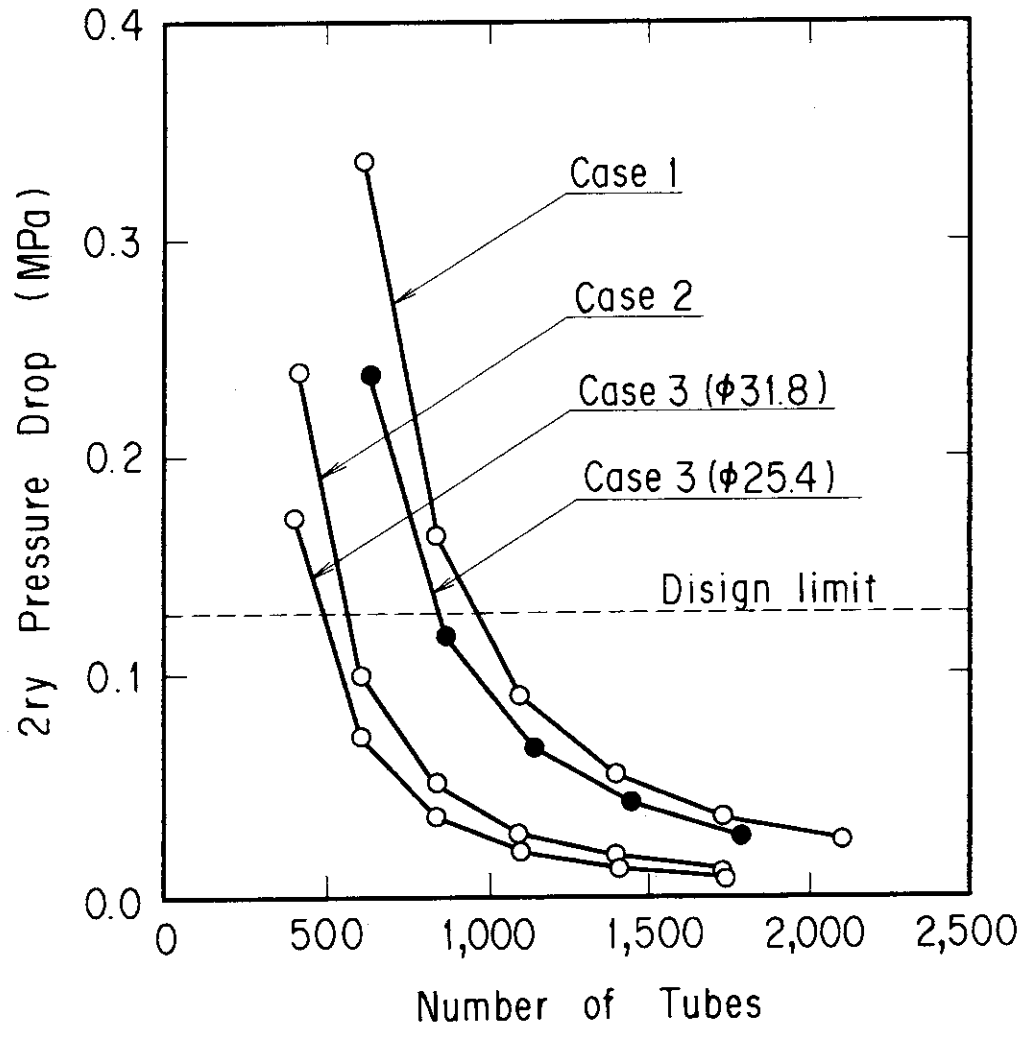

Fig.14. Pressure drop of secondary helium gas flow dependent on number of tubes.

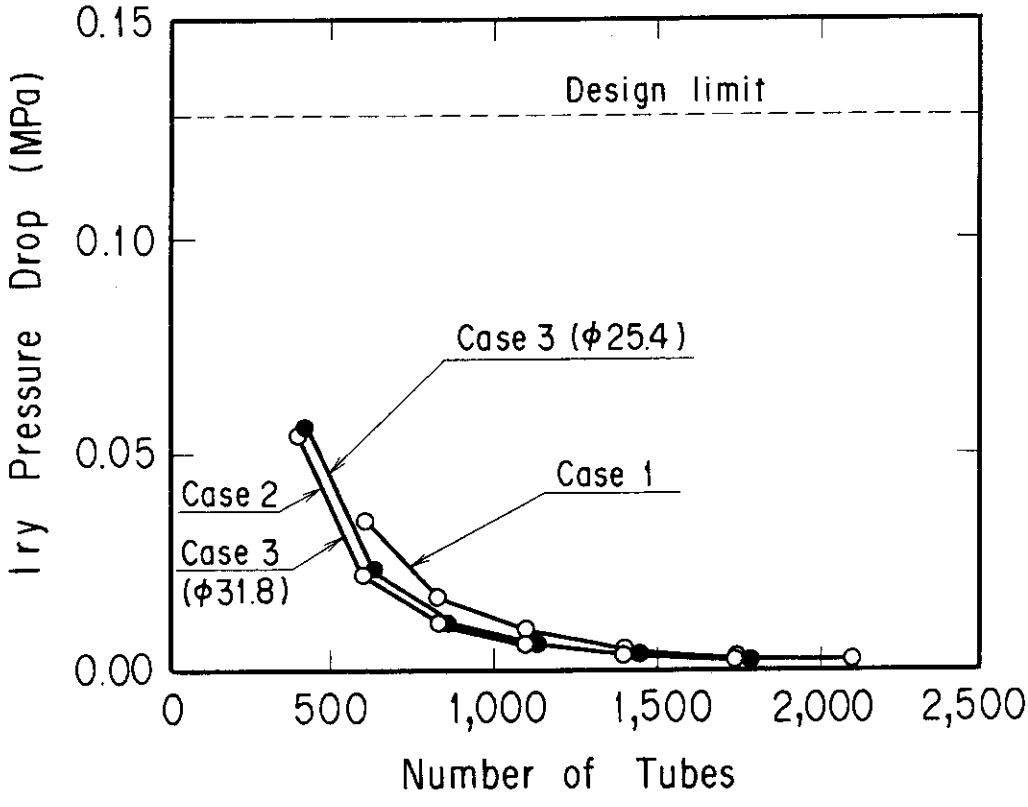

Fig.15. Pressure drop of primary helium gas flow dependent on number of tubes.

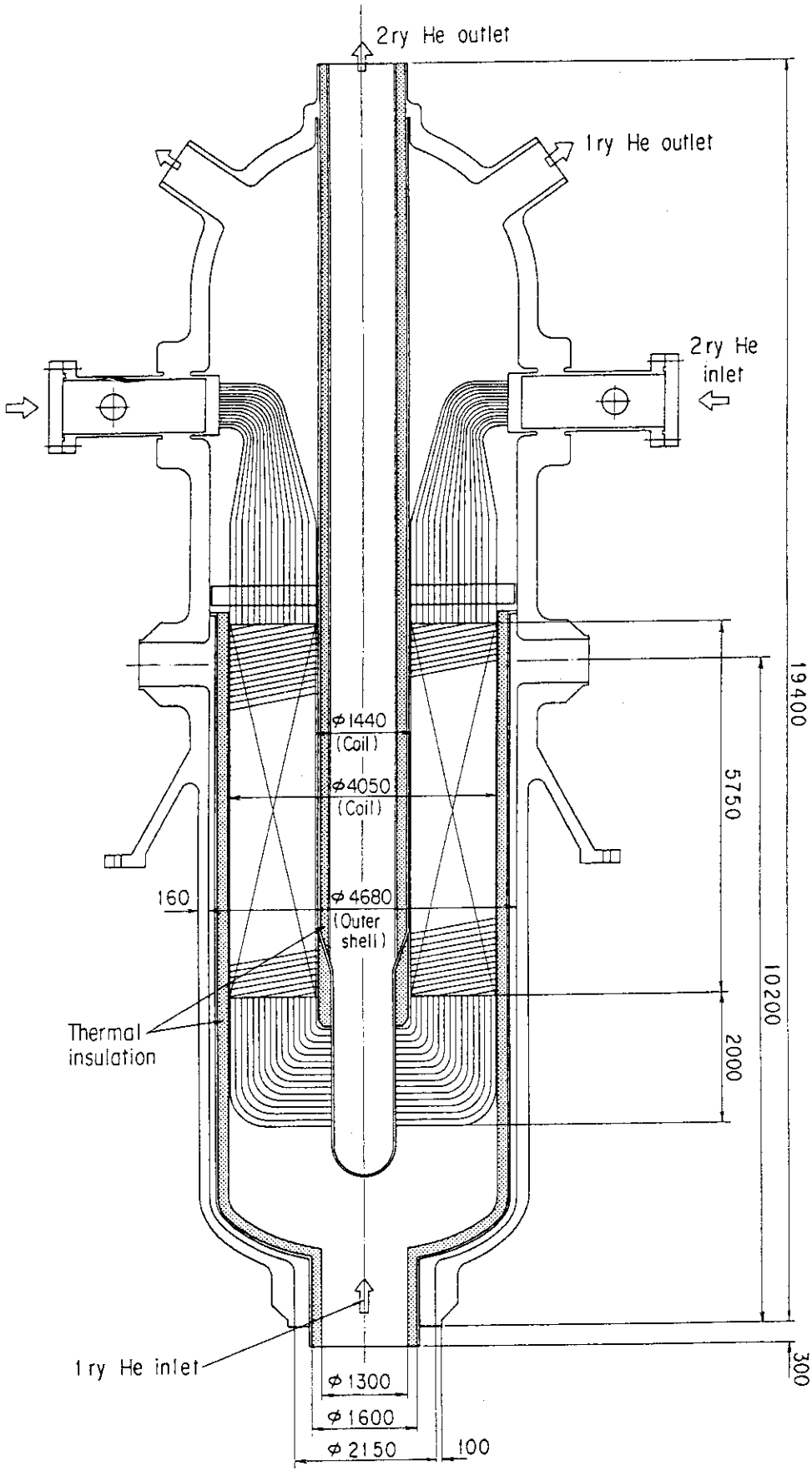

Fig.16. Vertical arrangement of 315 MW IHX.

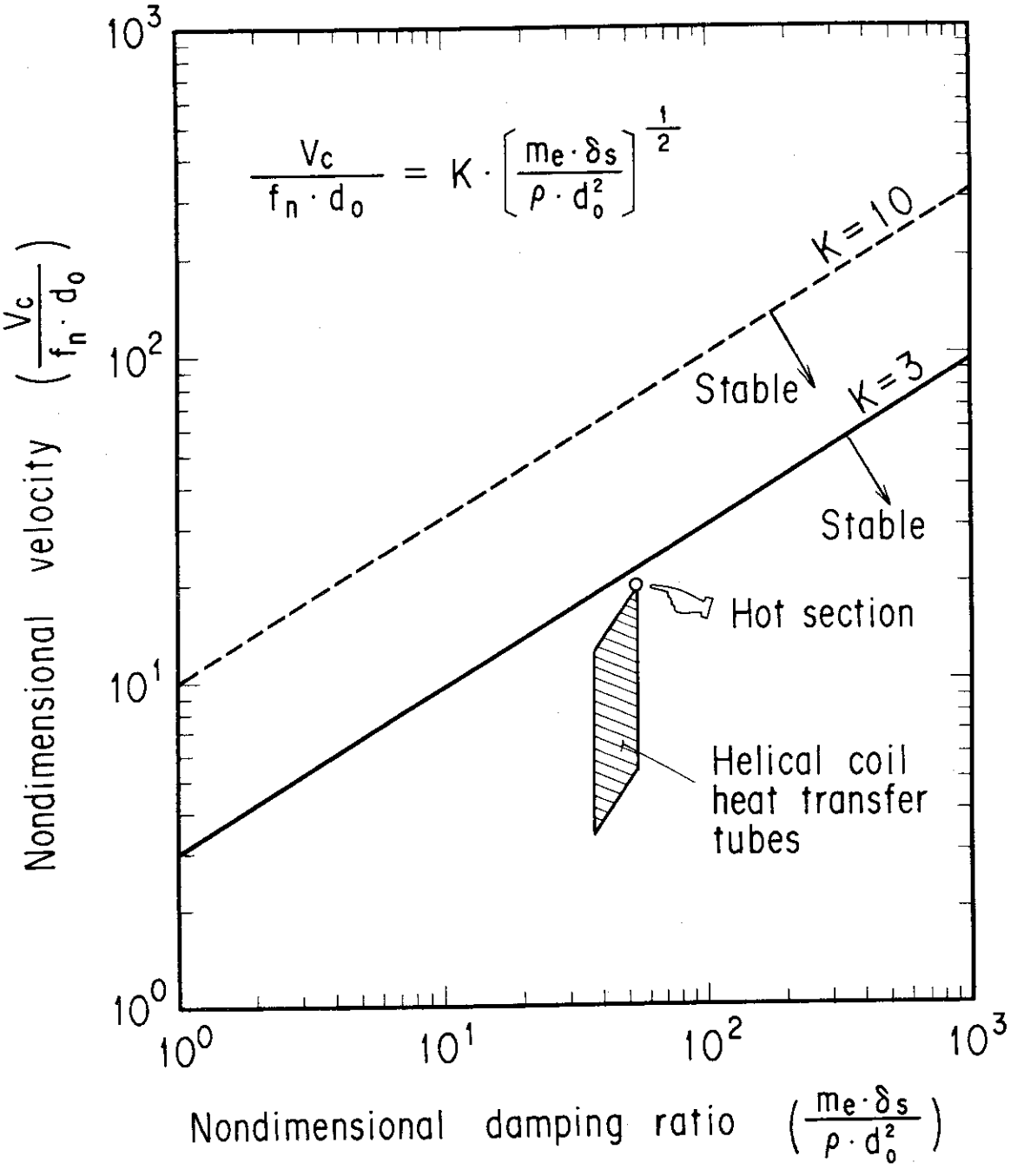

Fig. 17. Non-dimensional relationship showing a stability condition for the fluidelastic vibration.

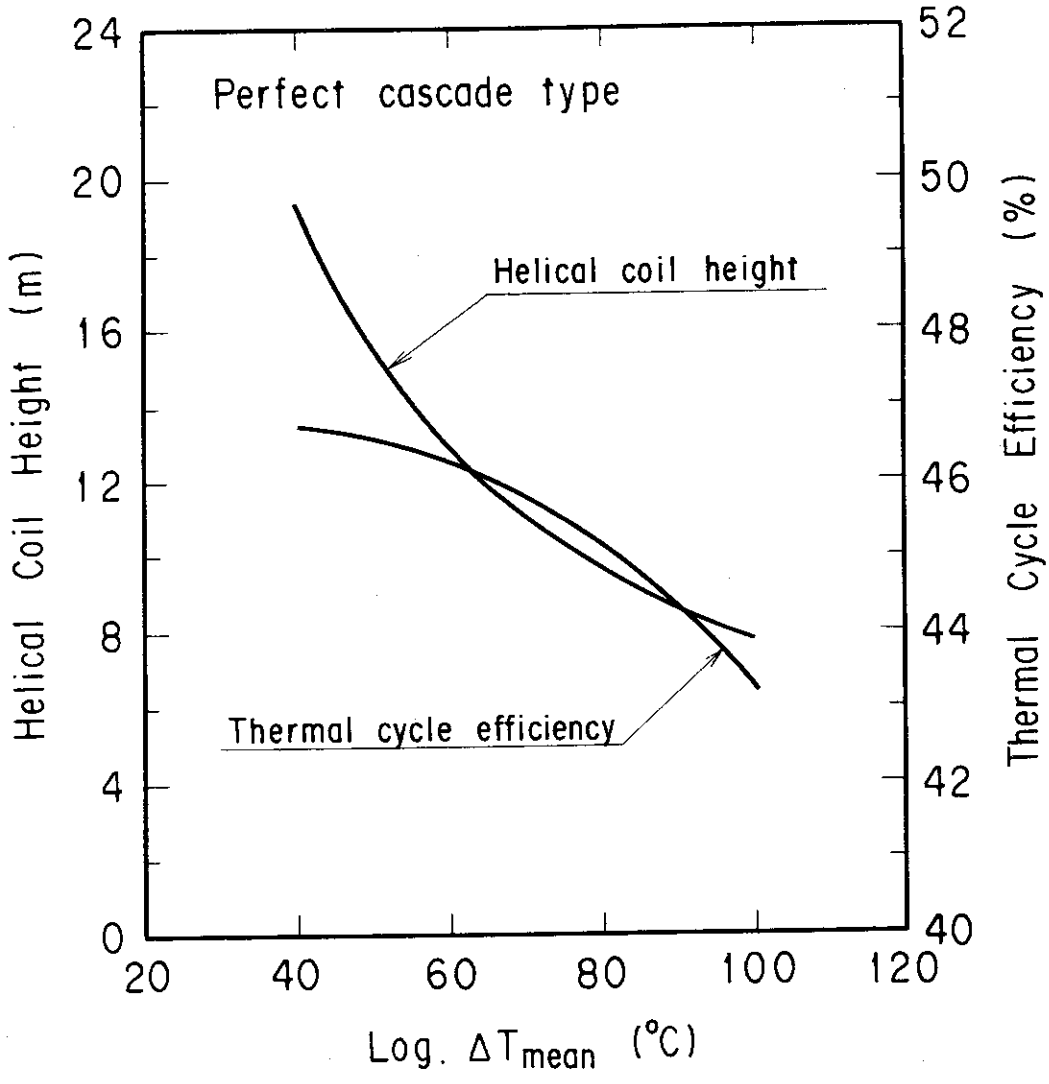

Fig.18. Dependence of helical coil height and thermal cycle efficiency on the logarithmic mean temperature difference of IHX in Case 1.

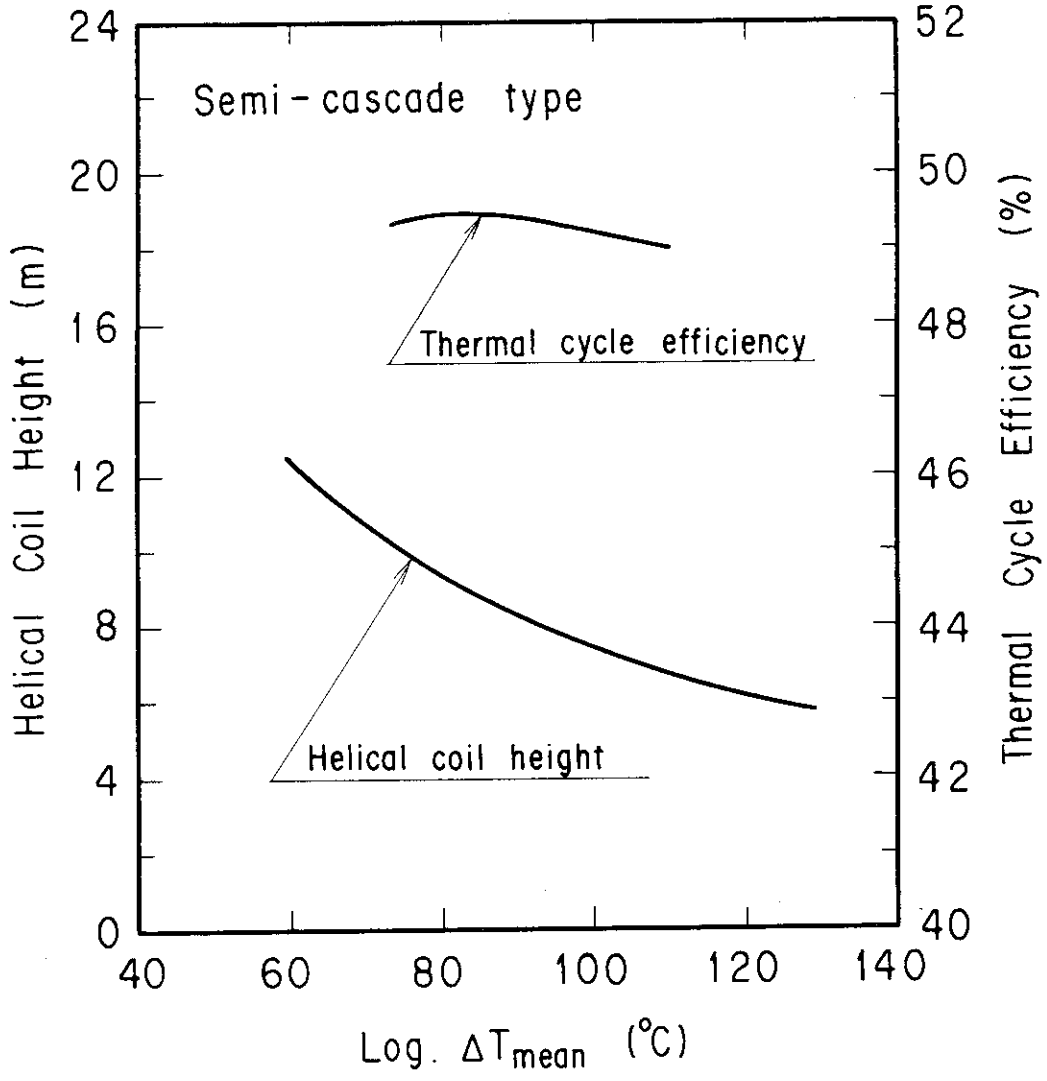

Fig.19 Dependence of helical coil height and thermal cycle efficiency on the logarithmic mean temperature difference of IHX in the Semi-cascade type similar to Case 2.